Chem Soc Rev

This article was published as part of the

2008 Gold: Chemistry, Materials and Catalysis Issue

Please take a look at the full table of contents to access the other papers in this issue

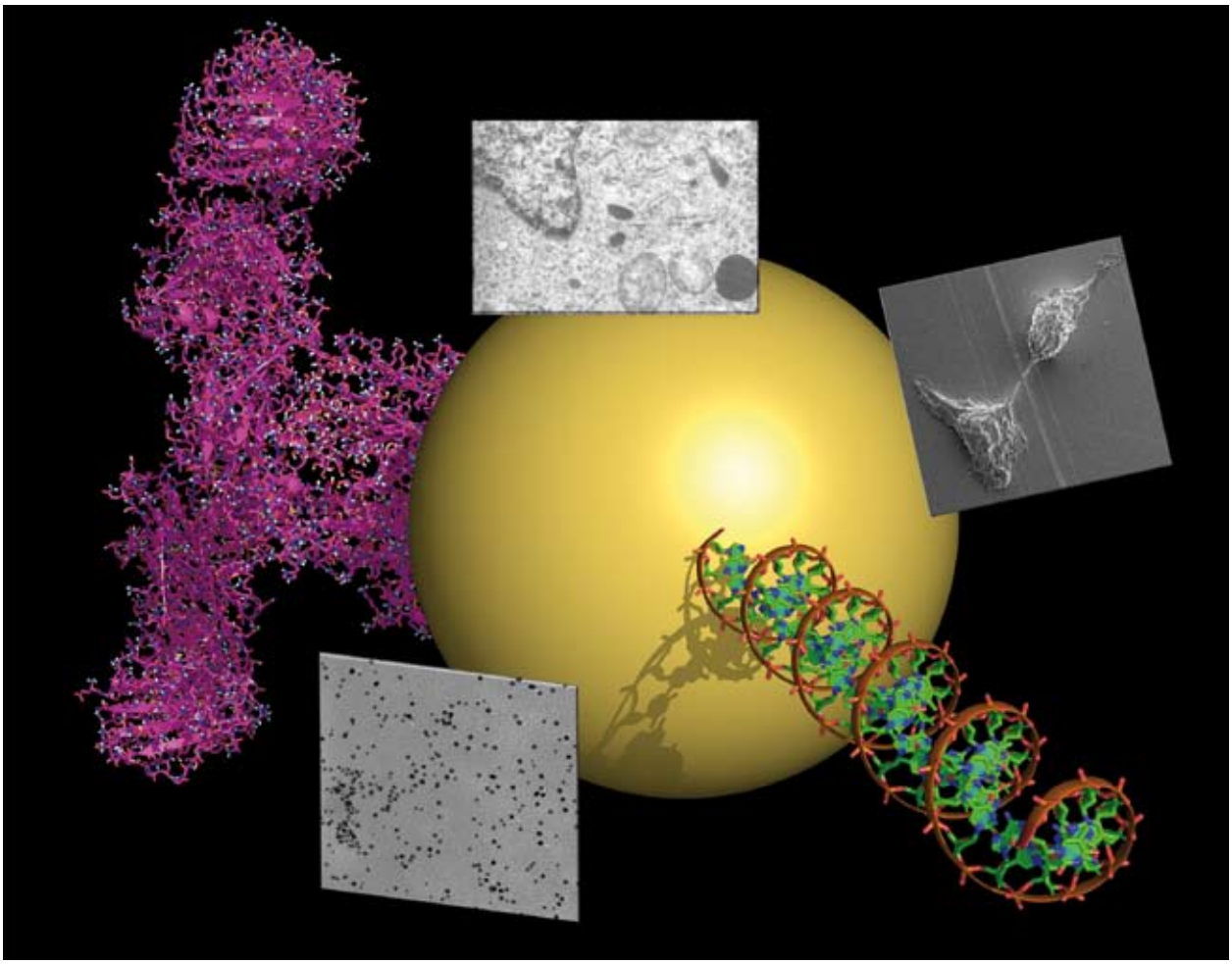

The use of gold nanoparticles in diagnostics and detection†

Robert Wilson

Received 25th March 2008
First published as an Advance Article on the web 16th July 2008
DOI: 10.1039/b712179m

The widespread use of gold nanoparticles (GNPs) as labels in diagnostics and detection is due to a unique combination of chemical and physical properties that allow biological molecules to be detected at low concentrations. In this *critical review* detection methods based on GNPs are divided up and discussed based on the way in which signals are generated in response to specific target molecules. Particular attention is devoted to methods that allow target molecules to be detected with the unaided eye because these, more than any other, harness the full range of properties that make GNPs unique. Methods that are discussed include those in which specific target molecules induce a visible colour change, chromatographic methods that allow non-specialized users to perform sophisticated tests without additional equipment and methods in which trace amounts of GNPs are rendered visible to the unaided eye by catalytic deposition of a metal such as silver. The use of metal deposition as a means of enhancing the signal for optical and electrical detection is also reviewed. The other detection methods included in this review are based on interactions between GNPs and molecules located in close proximity to their surface. These include methods in which light emission from such molecules is enhanced (surface enhanced Raman scattering) or quenched (fluorescence), and methods in which the accumulation of specific target molecules induce subtle changes in the extinction spectra of GNPs that can be followed in real time with inexpensive equipment (166 references).

Introduction

The practical use of colloidal gold as a pigment in glass dates back to at least to the fourth century AD when it was used to stain the Lycurgus cup, which is now housed in the British Museum, but contrary to what has sometimes been written the red colour of medieval stained glass is not due to the presence of gold nanoparticles or any other form of gold. In Europe the ability to make ruby glass (glass stained with gold nanoparticles) was rediscovered by the German chemist Johann Kunkell in the second half of the seventeenth century. His method involved adding gold nanoparticles precipitated from *aqua regia* to molten glass. Gold nanoparticles precipitated in this way are known as the Purple of Cassius after Andreas Cassius the younger who described a method for their preparation in his book *De Auro*, although a similar method had earlier been described by the German chemist Johann Rudolph Gauber. By the beginning of the eighteenth century, GNPs were also being used as a pigment in the decoration of porcelain (Fig. 1) and metalwork, and from Europe their use spread to China where they were used in the characteristic pink glaze of *Famille-Rose* porcelain during the Qing dynasty. Johan Kunkel is responsible for the first recorded speculation that the individual particles in colloidal gold were so small as to be invisible to the unaided eye, but it is unlikely that he ever conceived of just how small they really were. Nor is it likely that he ever imagined that the same thing that imparted such a deep red colour to the products of his glass factory would one day be used to diagnose all manner of diseases and help predict their outcome. Like the Roman glassmaker who made the Lycurgus cup, he would have known that only trace amounts of gold were needed to impart this colour, and he would have noticed that the glass looked different in reflected and transmitted light, but he knew nothing about how the gold interacted with light to produce the rich colours that he and his customers so admired. In our own time this same colour is seen by thousands of people every day when they carry out simple diagnostic tests in which infinitesimal quantities of unseen molecules are rendered visible to the unaided eye by what we now know are nanometre sized particles of gold.

Department of Chemistry, Liverpool University, Liverpool, UK L69 7ZD

† Part of a thematic issue covering the topic of gold: chemistry, materials and catalysis.

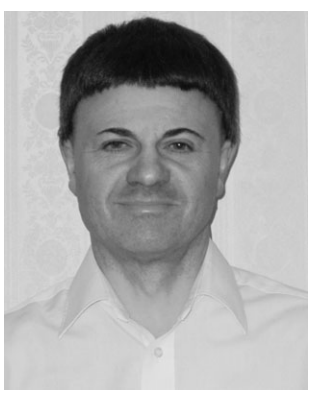

Robert Wilson

Robert Wilson obtained his PhD from Cranfield University where he conducted research on immunoassays and biosensors. Later, at Liverpool University, he researched the analytical applications of electrochemiluminescence, and detection methods based on micro- and nano-particles. His current research includes the use of nanoparticles in multiplexed detection, lateral flow diagnostic devices and layer-by-layer self-assembly.

Fig. 1 Porcelain jug made at Meissen, Germany, in about 1740. The red colour of the decoration is due the presence of gold nanoparticles in the glaze. The same colour is seen every day by the users of diagnostic tests in which gold nanoparticles render trace amounts of target molecules visible to the naked eye. Picture courtesy of the Victoria and Albert Museum, London.

Gold nanoparticles (GNPs) can be prepared in a broad range of diameters (2 to 250 nm) with a high degree of precision and accuracy. Once prepared, they are stable for long periods, and because they are generally employed at very low concentrations they are economic to use even though the material from which they are made is proverbially expensive. They are easily functionalized with recognition molecules (antibodies, antigens, oligonucleotides, *etc.*) by methods that lead to highly stable conjugates, and provided these are properly blocked non-specific interactions with other surfaces can be reduced almost to zero. Their intense red colour is due to the interaction of incident light with a collective oscillation of free electrons in the particles known as localized surface plasmon resonance. The extinction cross-section of the particles, and the wavelengths at which they absorb and scatter light, depends on their size and shape, the dielectric properties (refractive index) of the surrounding medium and their interactions with neighbouring particles. For spherical particles with a diameter of 10 nm the colour seen in transmitted light is due almost entirely to absorbance, but as the diameter increases scattering becomes increasingly significant; the ratio of scattering to absorbance for 100 nm particles is several hundred times greater than for 10 nm particles. The increase in diameter is also accompanied by an increase in the extinction coefficient and a red shift in the plasmon band that eventually moves into a region of the electromagnetic spectrum where the human eye is less sensitive. The net result is that particles with a diameter of around 80 nm are most visible to the human eye. Particles with this diameter have an extinction coefficient of around 5×10^{10} M^{-1} cm^{-1}. This compares favourably with the extinction coefficients of organic dyes that are typically four or five orders of magnitude lower, but a more meaningful comparison is with dyed latex microspheres of similar (slightly larger) diameter. These have similar extinction coefficients to GNPs, but they are more expensive to purchase, and more difficult to make in-house and conjugate to recognition molecules. The widespread use of GNPs in detection and diagnostics is due to a combination of low cost, ease of conjugation and unusual optical properties rather than the latter alone. Unlike fluorescent dyes, their optical properties are not altered by prolonged exposure to light, which allows results of diagnostic tests to be archived directly rather than in electronic form.

The use of gold in healthcare dates back many centuries. In medieval Europe *aurum potabile* (drinkable gold) was invested with the power to cure a diverse range of diseases, but because it was prepared by simply quenching a piece of the heated metal in wine it is unlikely that it contained much if any gold. It was not until the sixteenth century that European alchemists began to use *aqua regia* as a means of dissolving gold, but even then it was various forms of gold chloride rather that GNPs that were used in medicine. By the eighteenth century, the use of gold in medicine was generally frowned upon although its use continued into the nineteenth century, most notably as a treatment for syphilis, alcoholism and tuberculosis. Treatment of the latter at least had some scientific foundation and, although it never resulted in a cure for tuberculosis, it did lead to the observation that gold compounds were effective in the treatment of rheumatoid arthritis, a purpose for which gold remains in use to the present day as the active ingredient in the drug Aurofin. The first verifiable use of GNPs in diagnostics did not occur until the early twentieth century when Lange used a variation of the Zsigmondy flocculation test to identify altered proteins in the cerebrospinal fluid of patients with syphilis.[1,2] Later reports claimed that other morbid conditions of the central nervous system could also be diagnosed, but because of their unreliability none of these tests are still in use today. More recently GNPs conjugated to antibodies and other recognition molecules have been used as labels in electron microscopy and,[3,4] following the introduction of GNP catalysed silver enhancement, in light microscopy.[5,6] These developments have been dealt with elsewhere and this review will focus primarily on the use of GNPs as labels in diagnostics and detection.

Separation-free methods of detection

The sensitivity of any detection method is determined by the lowest signal that can reproducibly be distinguished from the background. Maximum sensitivity is achieved when all experimental errors that contribute to unwanted variations in this signal are eliminated. A major source of variation in any detection scheme are the errors that accumulate during addition and separation steps, and therefore sensitivity can be improved by reducing the number of these steps to a minimum. This also facilitates automation and improves accessibility to untrained users. These advantages have contributed to the popularity of separation-free detection methods, but sensitivity is often compromised by high background signals. This is the case with GNPs where an inability to distinguish small spectral shifts against a much larger background imposes a lower limit on sensitivity of around 0.2 nM on

detection by the unaided eye, although this can be improved by several orders of magnitude with instrumental detection.

Distance dependent detection of antigens

The mean distance between GNPs in a typical sol is greater than 1000 nm. At this distance there is no significant overlap between the dipoles of neighbouring particles, but when this distance is reduced to less than the diameter of the particles overlap induces colour changes as shown in Fig. 2A. These distance dependent colour changes were first exploited for detection by Leuvering and co-workers who developed a series of sol particle immunoassays (SPIA's) for target molecules in urine and serum.[8–10] In the separation-free version of this approach GNPs conjugated to antibodies are cross-linked (agglutinated) by multivalent binding to target molecules (Fig. 2B). At high concentrations of target molecule there is a visible colour change from red to blue, but at lower concentrations this change can only be detected with instruments such as a spectrophotometer. Sensitivity has subsequently been improved by using more advanced instrumental techniques such as hyper-Raleigh scattering (HRS) and differential light-scattering spectroscopy (DLSS),[11,12] and the approach has been extended to monovalent molecules by conjugating analogues of them to the GNPs, or a carrier molecule such as BSA (bovine serum albumin).[13–15] In their original work Leuvering and co-workers observed a visible colour change when they sandwiched high concentrations ($\sim$0.1 nM) of low molecular weight target molecules (37 kDa) between 60 nm GNPs conjugated to antibodies because the distance between the particles ($\sim$25 nm) was significantly less than their diameter. Fig. 2C shows the relationship between GNP diameter and the size of some common target molecules. The minimum distance between two particles conjugated to antibodies with a molecule such as ferritin sandwiched between them is about 45 nm and therefore only a small colour change is observed even when large particles are used. For many years the sensitivity of SPIA's in

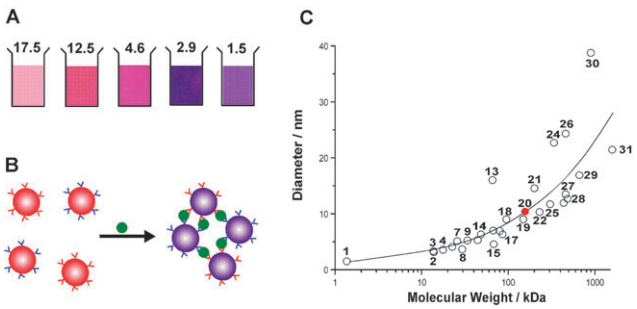

Fig. 2 (A) Effect of inter-particle distance in nanometres on the colour of 15 nm GNPs seen in transmitted light; colours derived from ref. 7, copyright American Chemical Society. (B) Schematic diagram of distance dependent sandwich assay for high molecular weight polyvalent antigen (green circles) leading to agglutination of GNPs and a red shift in their extinction spectrum. (C) Graph of GNP diameter *versus* molecular weight for a range of common antigens (reprinted from ref. 16 with permission from Elsevier). The red circle indicates the position of immunoglobulin-G antibodies that are common to all distance dependent methods of detecting antigens. The identities of other molecules in this graph can be found in ref. 16.

undiluted serum or urine samples was compromised by apparently random variations in the background signal,[17] but these were eventually traced to refractive index induced changes in the extinction spectrum caused by non-specific binding, which were then eliminated by better optimisation of the conditions.[18,19] More recently distance dependent immunoassays have been carried out with gold nanoshells. Each nanoshell consists of a silica core surrounded by a thin shell of gold. By tuning the relative dimensions of the core and shell the extinction maximum can be systematically varied from 700–1300 nm. One advantage of this is that the extinction maximum can be tuned to a wavelength at which interference from absorbing molecules in blood and other matrices is minimal. Hirsch and colleagues fabricated gold nanoshells consisting of a 96 nm diameter core surrounded by a 22 nm shell and used them to carry out distance dependent immunoassays in dilute serum.[20]

Distance dependent detection of nucleic acids

While many antigens are too large to produce a significant change in the extinction spectrum when they are sandwiched between GNPs, each base pair in double stranded DNA only contributes a distance of 0.34 nm and therefore nucleic acids are far more amenable to detection. Distance dependent changes are the basis of the well-known colorimetric detection of nucleic acids that was first reported by Mirkin and coworkers.[21,22] In this method single stranded target (linker) sequences are sandwiched between GNPs conjugated to thiolated reporter oligonucleotides. This is accompanied by a colour change from red to purple that is reversed on increasing the temperature. The rate and extent of this colour change depends on the length of the linker sequence, with longer sequences inducing smaller shifts in the extinction spectrum that take longer to appear.[23] A visual record of the reverse colour change can be obtained by removing aliquots and spotting them onto a C18 reverse-phase thin-layer chromatography plate as the temperature is increased (Northwestern spot test).[22] For a given sequence, the temperature at which the reverse colour change (melting) takes place depends primarily on the salt concentration, but is also influenced by the distance between the particles and the density of oligonucleotides attached to them;[24] it is always higher than the melting temperature of the corresponding duplex without GNPs. The exact temperature at which the colour change takes place is thought to depend on a mechanism in which the melting of one linker sequence promotes the melting of others.[24] It has been reported that this mechanism induces melting temperatures that are substantially narrower than those observed in conventional assays,[25–27] but a comparison with high resolution melting point curves based on fluorescent dyes[28,29] shows that this is not always correct. Murphy and Redmond have developed a compact instrument for melting curve analysis of GNP conjugates in small volumes of sample,[26] and Shen and coworkers have used distance dependent detection to detect single base polymorphisms (SNPs);[30] SNPs are the most abundant form of genetic mutation and their identification is important in medical diagnostics, disease prevention and prognosis. In the method reported by Shen, genomic target

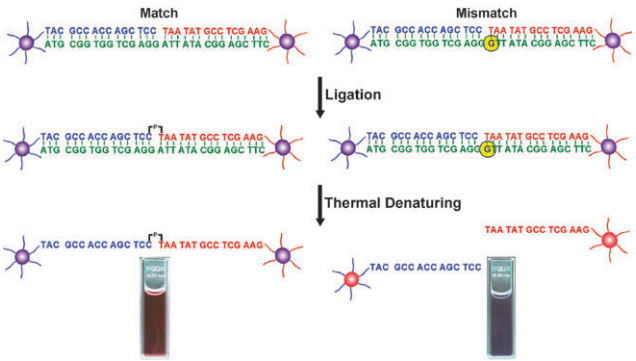

Fig. 3 Distance dependent detection of single base imperfections in DNA. At low temperature the extinction spectra of GNPs linked by matched and mismatched sequences are red-shifted, but only the former are substrates for DNA ligase. The latter, because the target sequence contains a single base mismatch (yellow circle), are not joined by the enzyme and therefore the red-shift in their extinction spectrum can be reversed by heating.

sequences were sandwiched between GNPs conjugated to oligonucleotides and treated with a high fidelity DNA ligase as shown in Fig. 3. When the target sequence was a perfect match for the capture sequences the GNPs were covalently linked together and the sol remained purple on heating, but when there was a mismatch the colour changed to red. More recently Qin and Yung have quantified SNPs using a combination of gel electrophoresis and GNPs conjugated to single oligonucleotides.[31] Distance dependent detection with GNPs is not sensitive enough to detect nucleic acids at the concentrations that are normally present in biological matrices and therefore it must be combined with some form of amplification technique such as PCR (polymerase chain reaction) or silver enhancement before it can be applied to real samples.

Distance dependent detection of amplified nucleic acids

PCR is the most widely used amplification technique in molecular biology, but it has never been successfully combined with GNPs for single-step separation-free detection. The possibility of using oligonucleotides conjugated to GNPs as primers has been demonstrated,[32] but Taton and co-workers have shown that monothiolated oligonucleotides dissociate from GNPs and degrade at elevated temperature.[33] At 95 °C (a temperature often used to denature double stranded DNA in PCR) around 35% of the oligonucleotides dissociated after thirty minutes, but even when dissociation approaches 100% the particles do not precipitate, probably because they are stabilized by direct interaction with DNA bases. One solution to thermal instability is to conjugate oligonucleotides to GNPs by more than one anchoring thiol.[34–36] This certainly enhances stability, but as yet there is no report describing how these improved conjugates perform under PCR conditions. An alternative solution to the problem of thermal instability is to perform the amplification at lower temperature. Isothermal amplification methods avoid high temperature,[37] but on closer inspection many of them are based on expensive cocktails of enzymes and generate unsuitable products. Nucleic acid sequence-based amplification (NASBA), for example, requires three enzymes and generates RNA products, which may

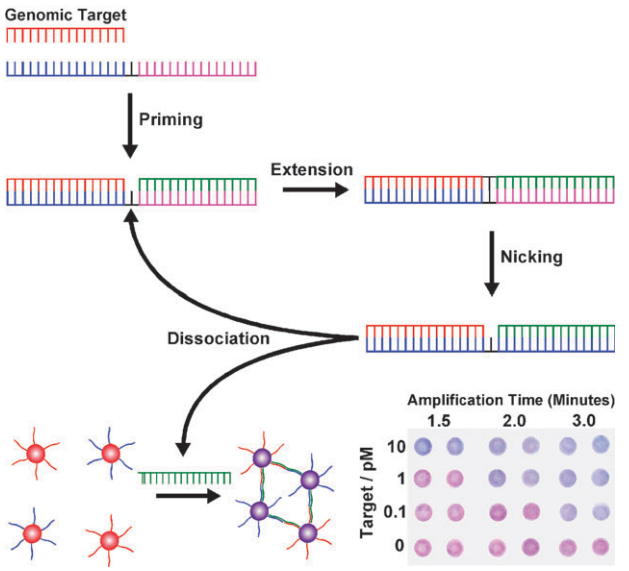

Fig. 4 Simplified scheme of the EXPAR (exponential amplification reaction) isothermal amplification method in which genomic target sequences are reformatted onto short linker sequences and amplified at a constant temperature of 55 °C. Northwestern spot tests (lower right hand corner) show the effects of time and target concentration on the colour of the GNPs; colours derived from ref. 38, Copyright American Chemical Society, which should also be consulted for full details of how exponential amplification is achieved.

contain secondary structures that interfere with hybridisation. There is currently only one example of an isothermal nucleic acid amplification technique that has been interfaced with GNPs and distance dependent detection.[38] In this method (Fig. 4) a trigger sequence is exponentially amplified at 55 °C and reformatted onto a linker oligonucleotide that agglutinates GNPs. The length and sequence of the linker were chosen for maximum colour change. This protocol achieves $>10^6$ fold amplification in under 5 min and allows target concentrations down to100 fM to be detected with the unaided eye. In recent work the trigger sequence was excised from genomic DNA derived from herpes simplex virus.[39]

Distance dependent detection with aptamers

Aptamers are nucleic acid sequences that have been selected from combinatorial libraries by the SELEX process.[40] Their structural and chemical properties allow them to recognize molecules other than nucleic acids in much the same way that antibodies recognize antigens. They are easier to produce than antibodies and more stable in the face of harsh conditions. For some target molecules, especially those with a low molecular weight, they are reported to perform as well as or better that antibodies. The first report describing their combination with GNPs was by Willner and co-workers who showed how thrombin could be detected by sandwiching it between particles conjugated to thiolated aptamers.[41] There was no colour change, but agglutinated GNPs were selectively precipitated with a centrifuge leading to a change in optical density proportional to the amount of thrombin in the sample. Chang and co-workers used a similar approach to detect platelet-derived growth factor (PDGF), but they did observe a colour

change.[42] Methods based on aptamers conjugated directly to GNPs can only detect target molecules that are able to accommodate at least two aptamer binding sites. Liu and Lu have reported a more general approach that is also suitable for low molecular weight molecules with only one binding site.[43] A suspension of GNPs conjugated to thiolated oligonucleotides changes colour from red to purple when they are agglutinated by aptamer sequences, but when target molecules are added they bind to the aptamer and the colour change is reversed as shown in Fig. 5.

Distance dependent detection of enzymatic reactions

Enzyme activity can be determined with substrates that lead to aggregation or dissociation of GNPs. Scrimin and co-workers reported a general method for measuring protease activity in which GNPs are linked by a substrate peptide terminated at either end with cysteine.[44] The peptide is incubated with the sample and then the products are mixed with GNPs. Peptides that have not been cut by a protease agglutinate the particles leading to a colour change as shown in Fig. 6. The method has been used to detect nanomolar concentrations of thrombin and lethal factor Xa from *Bacillus anthracis*. Brust and co-workers determined the activity of kinase enzymes using GNPs capped with peptides.[45] Enzyme catalysed transfer of biotin from γ-biotin–ATP to the particles was indicated by a colour change when streptavidin was added. The method was used to estimate the IC_{50} values of three potential kinase inhibitors in a multiwell plate. DNAzymes are catalytic nucleic acid sequences that are obtained by selection from combinatorial libraries.[46] Liu and Lu used GNPs to detect the reaction of a metal-dependent DNAzyme.[47] The particles were linked by a substrate sequence that was cut by the DNAzyme when Pb^{2+} was added leading to a change in colour from blue to red. Micromolar amounts of lead ions were detected in less than 10 min. Li and co-workers developed an assay for alkaline phosphatase activity based on the ability of adenosine phosphate capping ligands to prevent salt induced flocculation of GNPs.[48] The stability of GNPs capped with these ligands decreases in the order ATP > ADP > AMP and therefore the activity of alkaline phosphatase acting on adenosine phosphates can be determined from the extent of the colour change

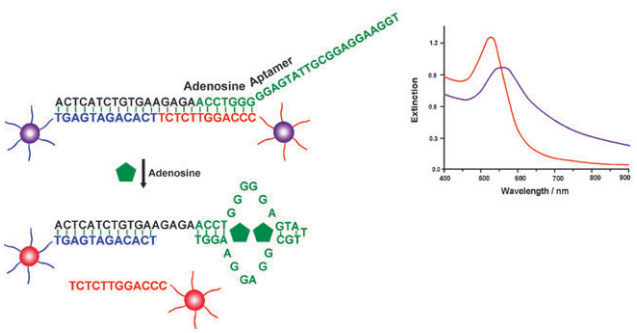

Fig. 5 Distance dependent detection of adenosine with an adenosine aptamer. In the absence of adenosine the extinction spectrum of the GNPs is red-shifted (purple line of inset graph) due to cross-linking, but on addition of adenosine this is reversed (red line of inset graph). Graph reprinted from ref. 43, copyright Wiley-VCH Verlag GmbH & Co.

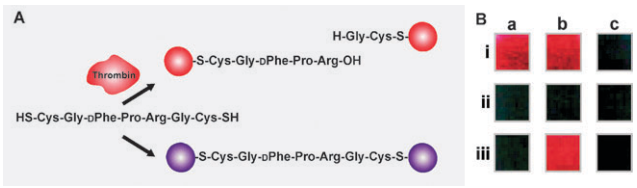

Fig. 6 Distance dependent detection of proteolytic enzymes. (A) In the absence of a substrate-specific protease (thrombin) GNPs are agglutinated by bivalent cysteine terminated peptides leading to a red-shift in their extinction spectrum. Cleavage of the peptide by thrombin prevents this. (B) Colours of GNP suspensions after exposure of the peptide substrate to the following cocktails of proteolytic enzymes: (ia) chymotrypsin, plasmin factor Xa and thrombin; (ib) chymotrypsin and thrombin; (ic) chymotrypsin, factor Xa and plasmin; (iia) factor Xa and chymotrypsin; (iib) chymotrypsin; (iic) factor Xa; (iiia) no enzymes; (iiib) thrombin; (iiic) plasmin; colours derived from ref. 44, Copyright The National Academy of Sciences of The United States of America.

from red to purple that occurs when citrate stabilised GNPs are added to the products of the reaction.

Distance dependent detection without a linker

Maeda and co-workers found that GNPs conjugated to thiolated oligonucleotides precipitated at high NaCl concentrations in the presence of complementary target sequences, but that a single terminal base mismatch could prevent this.[49] Later they showed how this could be used to detect single base polymorphisms (SNPs) that are important in the prognosis and diagnosis of cancer.[50] Genomic DNA was amplified by PCR and then the purified products were interrogated with base specific primers. The terminal base of PCR primers is very sensitive to mismatches; primers that are not matched have a much lower probability of being extended. In the method developed by Maeda and co-workers,[49] mismatched primers that were not extended had a one base overhang that prevented precipitation of GNPs as shown in Fig. 7. Li and co-workers found that GNPs conjugated to short (12-mer) single stranded oligonucleotides became more resistant to salt-induced flocculation when they were hybridised to 32-mer adenosine-binding DNA aptamer.[51] The addition of adenosine led to dissociation of the aptamer from the particles and induced a colour change that allowed low millimolar concentrations of adenosine to be detected in under 10 min. Thiolated nucleic acids are expensive and the method for conjugating them to GNPs requires a large excess of them beyond the amount that actually becomes attached to the particles. Li and Rothberg avoided this expense by detecting nucleic acids with citrate-stabilized GNPs.[52] First the sample was mixed with single stranded reporter sequences and then citrate stabilized GNPs were added. Single stranded nucleic acids prevent salt induced flocculation of GNPs because their exposed bases bind to the particles. In the absence of a complementary target sequence therefore the GNPs remain red, but when target sequences are present double stranded products are formed and the particles aggregate. The presence of a target sequence therefore is indicated by a colour change from red to blue. The key problem is how to link this colour change to meaningful nucleic acid detection. In later work Li and Rothberg

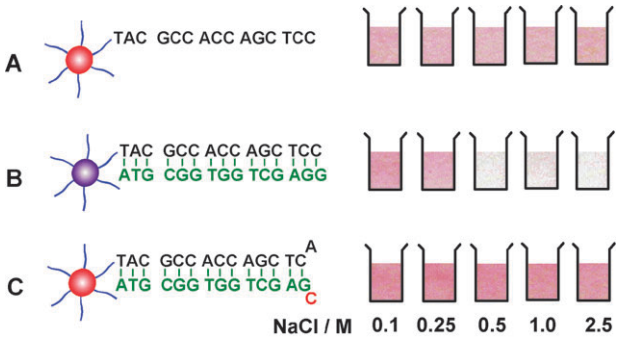

Fig. 7 GNPs conjugated to single stranded oligonucleotides are stable at high salt concentrations (A), but when they are hybridised to a complementary sequence they precipitate (B). Because a single base terminal mismatch is enough to prevent blunt end formation (C) single nucleotide polymorphisms (SNPs) can be identified; colours of GNP suspension derived from ref. 49, Copyright American Chemical Society.

described a method in which reporter sequences were hybridised to PCR amplicons,[53] but it is not clear how interference from the unextended primers was avoided. The authors say that these were removed by annealing to amplified products, but the concentrations of unextended single stranded primers at the end of a typical PCR reaction is usually several orders of magnitude higher than the concentration of amplified products so this would not normally be possible. More recently the same authors have used their method to detect RNA sequences,[54] but real samples contain many single stranded sequences other than the target and presumably these would prevent any colour change.

Size dependent detection of enzyme reactions

Enzymes that produce reducing agents can be detected by the growth and formation of GNPs. Willner and co-workers detected micromolar concentrations of glucose by enzyme catalysed enlargement of small gold nanoparticles.[55] The oxidation of glucose by glucose oxidase produces equimolar amounts of H_2O_2. The latter reduces $AuCl^{4-}$ to Au^0 leading to an increase in the size of the small GNP seeds and the formation of new ones. This is accompanied by a measurable change in the extinction spectrum proportional to the amount of glucose in the sample (Fig. 8). A similar approach has been used to detect micromolar amounts of neuro-transmitters[56] and inhibitors of acetylcholine esterase. In the latter example inhibitors prevent the enzyme from producing a reducing agent that catalyses the growth of GNPs.[57]

Refractive index dependent detection

Surface plasmon resonance (SPR) occurs when light incident on a metal surface excites surface electrons into a propagating wave known as a surface plasmon polaritron. Instruments using SPR to detect biomolecular interactions at planar macroscopic gold surfaces were first introduced in the 1990's.[58] In the configuration most often used for sensing, a glass substrate coated with a thin film of gold (~50 nm) is located at the interface between a prism and the sample as shown in Fig. 9. Light reflected from the gold shows a sharp

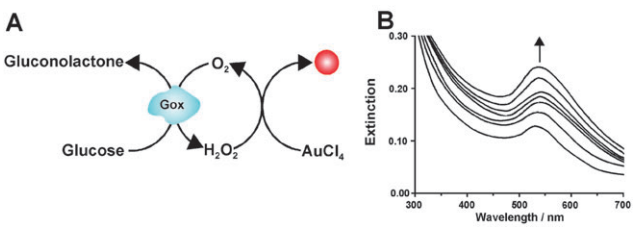

Fig. 8 (A) Glucose oxidase produces stoichiometric amounts of H_2O_2 when it oxidizes glucose, and H_2O_2 reduces gold cations to metallic gold. Deposition of the latter on GNPs produces an increase in extinction in proportion to the amount of glucose as shown in (B); graph reprinted from ref. 55, Copyright American Chemical Society.

drop in intensity when it couples with conducting electrons in the metal and sets up a strong evanescent wave that decays exponentially into the sample. The wavelengh at which the intensity drops to a minimum is highly sensitive to refractive index changes in the region occupied by the evanescent wave. These changes can be monitored by tracking the angle (θ in Fig. 9A) that corresponds to the minimum intensity of reflected light. For sensing purposes the gold film in contact with the sample is normally coated with capture molecules that promote the accumulation of specific target molecules in the region interrogated by the evanescent wave. Because this region only extends to a maximum of about 200 nm into the sample it can be monitored independently of the bulk solution. This allows specific binding reactions taking place at the surface to be followed in real-time without a separation step. Most biological molecules have similar refractive indices and therefore their effect on SPR is proportional to their mass. The sensitivity of conventional SPR biosensors is limited to around 1 pg of biological molecules per square millimetre of the sensing surface and therefore they are unable to detect low concentrations of small molecules (sensitivity for 20 kDa proteins is only about 1–10 nM). Sensitivity can be improved by sandwiching the target molecules between the sensing surface and a label that damps the surface plasmon wave. GNPs have often been used for this purpose because they produce a large change in the refractive index and couple with surface plasmon polaritrons in the gold film. Natan and colleagues

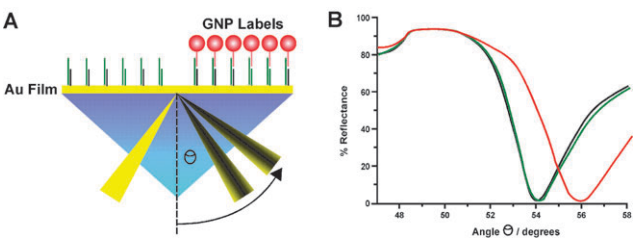

Fig. 9 (A) Conventional surface plasmon resonance (SPR) biosensors are often based on a thin film (~50 nm) of gold located at the interface between a prism and the sample. Low molecular weight (MW) molecules such as oligonucleotides produce very small changes in the deflection angle θ when they bind to the sensing surface (difference between the black and green lines in the graph (B)). When low MW target molecules are sandwiched between the surface and GNP labels much larger changes in the deflection angle are produced (difference between the green and red lines in graph (B)), but this also eliminates the key advantage of real-time label-free detection.

showed how GNPs could be used to improve the sensitivity of displacement assays for biotin,[59] and Keating and colleagues demonstrated a 1000-fold improvement in sensitivity for oligonucleotides,[60] but the introduction of a label into SPR eliminates its key advantage. Once this has been lost there are alternative detection methods, which in many cases are more sensitive and less expensive. The same is true of other techniques (quartz-crystal microbalances[61] and microcantilevers[62]) where GNPs have been used to improve sensitivity at the expense of label-free detection. Because the introduction of labels into conventional SPR eliminates its key advantage there are ongoing attempts to increase its sensitivity by other means. A sensing surface containing embedded GNPs absorbs light more efficiently that a surface composed entirely of gold and sets up a more intense evanescent wave. Chen and colleagues have exploited this to achieve a ten-fold increase in sensitivity by substituting a sensing surface composed of gold nanoclusters embedded in silica (SiO_2) for the planar gold film used in conventional SPR.[63]

The improved sensitivity of conventional SPR with GNP labels was among the observations that prompted Englebienne to investigate the possibility of using GNPs as the support in place of a macroscopic surface.[64] He showed that when GNPs conjugated to antibodies were mixed with the corresponding antigen there was a shift in the extinction spectrum that could be followed in real time at 600 nm with an ordinary UV/Vis spectrometer as shown in Fig. 10. This shift in the extinction spectrum is due to a change in the refractive index at the surface of the particles rather than overlapping dipoles, as was clearly demonstrated with GNPs conjugated to antibodies that were unable to participate in cross-linking. The absence of cross-linking eliminates interference from precipitation that is often a problem in distance dependent detection and the acquisition of results in real-time permits higher sensitivity than is possible in end-point methods. Refractive index dependent detection with GNPs is considerably less expensive than conventional SPR and can be extended to low molecular weight molecules such as polypeptides and haptens.[65] Although multi-channel instruments for conventional SPR have been made

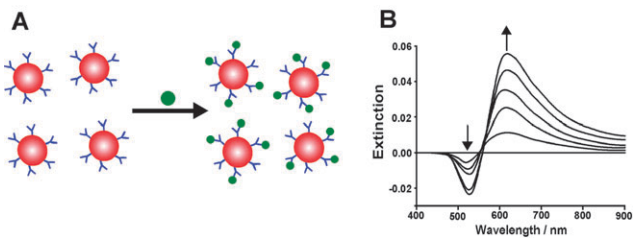

Fig. 10 (A) Scheme showing the effect of binding events on GNP conjugates in refractive index dependent detection. There is no cross-linking of the particles (compare with distance dependent detection in Fig. 2B) and no visible red-shift in the extinction spectrum. (B) Increases in extinction at 600 nm produced by (in order of increasing extinction at 600 nm) 2.8, 5.6, 11.2, 28 and 56 pmol of theophylline. Notice how small these increases are compared with those in distance dependent detection (see the graph in Fig. 5 for example), but sensitivity is high because the increase is followed in real time and because there is no interference from precipitation, which is sometimes a problem when particles are cross-linked. Graph reprinted from ref. 19, with permission from IOS Press.

they are too slow for high throughput applications such as lead structure identification in drug development, but multiple binding reactions are easily monitored in parallel with GNPs. Englebienne and co-workers used a clinical analyzer to screen up to 72 samples in parallel.[65] The absorbance of each sample was measured at 25 s intervals for a total of 20 min. Due to a high degree of automation it was possible to screen up to 3000 samples per day and potentially ten times this number could be screened with a more sophisticated instrument. No matter how precisely a batch of GNPs is synthesized the product will inevitably contain a range of diameters that obscure the small changes in extinction spectrum that occur in refractive index dependent detection and ultimately limit its sensitivity. Gold nanorods are particles with an aspect ratio (length divided by width) of greater than one. In addition to an extinction peak at around 530 nm they have a more intense peak at longer wavelengths arising from the plasmon oscillation of electrons along their longitudinal axis. The position of this peak can be shifted into the near infrared region by increasing the aspect ratio of the particles. The advantage of using longer wavelengths as a means of avoiding interference from absorbing molecules in matrices such as whole blood and serum has already been mentioned, but an additional advantage is that sensitivity to changes in the refractive index of the surrounding medium increases at longer wavelengths.[66] Chilkoti and colleagues used dark field microspectroscopy to track changes in scattering at 780 nm from a single nanorod in response to the binding of nanomolar concentrations of streptavidin.[67] Single particle methods such as this may allow stochastic sensors to be developed based on the detection of individual binding events in minute volumes of sample.

Nath and Chilkoti have also developed a hybrid solid phase version of refractive index based detection in which a monolayer of GNPs was immobilized on a glass substrate and placed in contact with a liquid sample.[68] Changes in the extinction spectrum of the GNPs in response to changes in the local refractive index were detected with an ordinary UV/Vis spectrometer. In one example the binding and dissociation of streptavidin to GNPs functionalized with biotin was followed in real time by monitoring the increase in absorbance at 550 nm. Molecularly imprinted polymers (MIPs) are synthesized by polymerization of appropriate monomers in the presence of a target molecule that becomes embedded in the matrix.[69] These embedded molecules are later released leaving behind complementary cavities that can later re-bind to the target molecule by a mechanism that resembles the binding of antibodies to antigens. Sugimoto and colleagues synthesized a MIP in the presence of 5 nm diameter GNPs and adrenaline that became swollen on exposure to target molecules.[70] This led to an increase in inter-particle distance and a blue-shift in the extinction spectrum. More recently the same group have coated a similar MIP onto a conventional SPR chip and demonstrated a tenfold increase in label-free sensitivity for the low molecular weight neurotransmitter dopamine.[71]

Fluorescence detection

Dual labeled oligonucleotides are widely used in real-time PCR.[72] In these probes the fluorescence of an organic dye is excited, or more often quenched, by close proximity to another

dye or quencher. Fluorescent dyes are also quenched by close proximity to GNPs. In recent work the quenching effect of GNPs on cyanine dyes,[73,74] and of gold (Nanogold) clusters on quantum dots (QDs)[75] at distances greater than 2 nm from the surface of the gold has been described, while in previous work the quenching effect at shorter distances has been reported.[76] Fluorescence enhancement has been detected from fluorophores placed at ~10 nm distances from a nanostructured metal surfaces, but this effect has not so far been observed for GNPs in suspension. Molecular beacons are dual-labeled oligonucleotide probes that comprise a stem–loop structure labeled at opposite ends with a fluorescent dye and a quencher dye.[72] On hybridization to a complementary nucleic acid sequence the fluorescent dye and the quencher are forced apart leading to an increase in fluorescence. Dubertret and colleagues replaced the quencher with a 1.4 nm diameter Nanogold cluster.[77] In the stem–loop configuration the dye was quenched by close proximity to the gold, but on addition of a complementary target sequence it was pushed away accompanied by an increase in fluorescence. The relative increase was up to an order of magnitude more than observed for conventional molecular beacons, but because Nanogold is not stable at high temperature these probes are not suitable for use in real-time PCR. Nanogold clusters have also been used as quenchers for dual-labeled probes based on QDs, but here they were reported to be no better than organic dyes.[78] More recently, however, Mattousssi and colleagues have investigated the quenching effect of Nanogold on QDs in more detail and shown that it operates over much longer distances than FRET (Förster resonance quenching transfer) quenching between organic dyes.[75] This potentially allows the development of dual labeled sensors for large molecules such as proteins. GNPs have also been used to quench QDs[79] and fluorescent dyes in displacement assays for proteins.[80] Rotello and colleagues prepared six sets of GNPs functionalized with a different inner-shell of hydrophobic, aromatic and polar groups and coated them with an outer layer of fluorescent polymer.[81] Because the distance between the polymer and the particles was very short fluorescence was strongly quenched. The GNPs were used to construct a two-dimensional sensing array in which each set of particles was confined to a different location in a multiwell plate (Fig. 11). When the array was contacted with protein solutions the extent to which the polymer was displaced depended on the affinity of a given protein for the inner shell. Thus each protein of the seven that were investigated produced a different pattern of increased fluorescence that was later used to decode the response produced by nanomolar concentrations of unknown proteins.

Methods of detection that involve separtion steps

Separation steps are carried out in a detection method to improve sensitivity. They are usually assisted by performing recognition reactions on some form of support that allows the products to easily be separated from unbound molecules and excess label. In the case of GNPs, a particular reason for performing a separation step to remove excess label is due to the poor ability of the human eye to distinguish between red and blue.[82] The effect of this on sensitivity is exasperated by

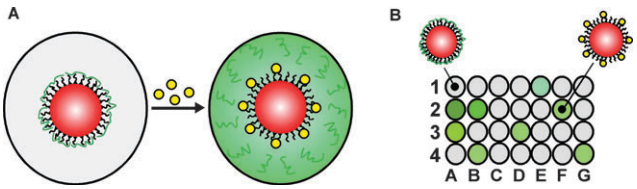

Fig. 11 (A) The displacement of fluorescent polymers from functionalized GNPs by protein molecules (dark green circles) leads to an increase in fluorescence. (B) Two-dimensional sensing arrays can be constructed by organizing sets of GNPs in a multiwell plate. Each row (1–4) contains a different set of GNPs, and each column (A–G) contains a different protein. Because the pattern of increased fluorescence is diagnostic of the protein it can be used to identify that protein in uncharacterised samples.

the lower extinction coefficients of agglutinated GNPs compared to those that are fully dispersed. Removal of excess unbound GNPs also allows the remaining bound particles to be enhanced by metal deposition. The most widely used metal deposition technique is silver enhancement.[83] Two solutions, one containing a silver salt such as silver nitrate and the other containing a reducing agent such as hydroquinone, are mixed and immediately applied to the GNPs. Metallic silver is preferentially deposited on the particles leading to an increase in their size and extinction that allows the products to be detected with relatively inexpensive imaging equipment, and in many cases to be seen with the unaided eye. Silver staining is a chemical amplification technique that in some respects resembles enzyme amplification. It is faster and more robust, but high quality results are only obtained when care is exercised to maintain clean solid supports and exert tight control over conditions such as time, temperature, pH and the concentrations of the staining reagents. Silver is precipitated by chloride ions and therefore these must be removed before silver enhancement, but washing with water is unsatisfactory because it leads to dehybridization of double stranded nucleic acids. Washing with sodium nitrate solutions containing sodium dodecyl sulfate (SDS) works well. Less well known, but reported to be superior, is enhancement by deposition of metallic gold on GNPs from solutions containing a gold salt ($HAuCl_4$) and hydroxylamine.[84]

Microsphere assays

The most accessible class of solid supports is microspheres. These are available in a wide range of sizes and surface chemistries from a variety of commercial sources. Minute amounts of GNPs bound to white microspheres are easily seen with the unaided eye by spotting them onto porous white supports or transferring them to a multi-well plate. The simplicity of microsphere assays and the ease with which high quality results can be obtained are important advantages, but because relatively large amounts of microspheres are required to produce a visible colour they can be also be expensive. The cost can be kept to a minimum by using microspheres with a large ratio of surface area to volume, but the diameter must be large enough to allow efficient separation. Polystyrene microspheres with diameters of 0.5 micrometres are a good choice because they have a high ratio of surface area to volume but are easily separated from unbound 10nm GNPs by filtration

or centrifugal precipitation. Letsinger and co-workers detected picomolar amounts of DNA by sandwiching it between capture oligonucleotides conjugated to white latex microspheres and reporter oligonucleotides conjugated to GNPs.[85] Results were visualized on a white porous support that was permeable to the GNPs, but retained the microspheres (Fig. 12). Microsphere assays for biotin and oligonucleotides in which the microspheres were visualized in a multiwell plate have also been reported.[86–88] The sensitivity of microsphere assays can be enhanced by silver staining GNPs retained on filters.[89] This allows nanogram amounts of specific genomic DNA to be detected without PCR. GNPs bound to magnetic microspheres are not visible against the brown background of the microspheres, but GNPs bound to them are easily removed from solution by magnetic separation thereby producing a change in the optical density proportional to the amount of target molecule.[90]

Planar supports

In solution phase assays with GNPs as the indicator it is not practical to detect more than one target molecule at the same time. To achieve this each test must be confined to a separate location that can be distinguished with the unaided eye or some form of imaging equipment. This can be done by organizing the tests into one- or two-dimensional arrays on a planar support. The planar supports most widely used with GNPs are glass, nitrocellulose, nylon and polyvinylidine difluoride. At high concentrations of target molecule, GNPs bound to glass supports are sometimes visible to the unaided eye, but for sub-nanomolar sensitivity the particles must be silver enhanced.[91] Sensitivity is improved by using glass supports coated with hydrogel surfaces such as CodeLink (GE Healthcare) and Nexterion® slide H (Schott). Materials such as nitrocellulose are porous membranes. Capture molecules such as antibodies and oligonucleotides are easily attached to these, and because they are white in colour and porous in structure they provide an ideal background for the visual detection of GNPs. Particles are visible to a depth of several micrometres and therefore minute amounts are capable of producing intense red spots or bands. Membranes that are more than a few microns thick are inefficient because GNPs beneath this depth are not visible. Glass slides coated with thin layers of nitrocellulose that eliminated this dead volume are now available from companies such as Whatman (FAST slides) and Schott (Nexterion® slide N). Metal deposition can also been used to enhance the signal from GNPs on porous membranes.[84,92]

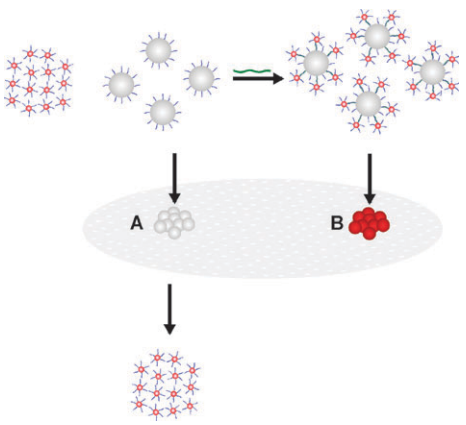

Fig. 12 Colorimetric microsphere assay with GNPs. (A) In the absence of target molecules white microspheres are retained on the filter and GNPs pass through. (B) In the presence of target molecule GNPs are bound to the microspheres, which then appear red when they are retained on the filter.

Lateral flow devices and immunoassays

Lateral flow devices (Fig. 13A) are one of the most important products of the diagnostics industry. They are easy to develop and inexpensive to manufacture in high volumes. Their popularity with users stems from their low cost and simplicity that allows non-specialized users to perform complicated tests at the point of need without additional equipment. Because they are supplied in dry form they can be stored at ambient temperature for long periods. In their most common form they consist of a porous white membrane striped with a line of antibodies or antigens, and interfaced with antibodies conjugated to a label that can be seen with the unaided eye. Most often that label is GNPs, but surprisingly, given their huge economic importance, very little of the research effort that has been devoted to GNPs has had any impact on these devices. There are a few reports describing lateral devices based on GNPs conjugated to oligonucleotides by one of the more recent methods,[93–95] but the vast majority of these devices are still based on GNPs conjugated to antibodies by a method that was first reported in 1979.[3] In this method, GNPs are mixed with an excess of antibodies, some of which then become attached (conjugated) to the particles by a poorly understood process that is believed to involve a combination of electrostatic, covalent and hydrophobic interactions. GNP conjugates produced in this way are generally quite stable, but there have been reports describing subsequent desorption of the antibodies,[96,97] and it is widely known that certain types of monoclonal antibody are not amenable to conjugation in the first place. Most of the detection methods that are currently carried out with lateral flow devices are immunoassays that depend on the recognition properties of antibodies. Competitive immunoassays are usually performed with the aim of

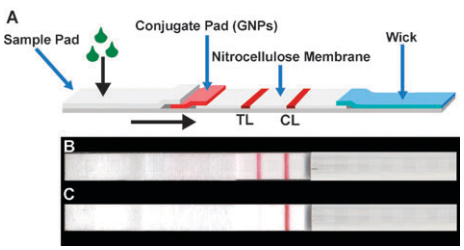

Fig. 13 (A) Design of a lateral flow device showing how the four main components (sample pad, conjugate pad, nitrocellulose membrane and wick) are interfaced by lamination. TL = test line and CL = control line. (B) Result of competitive assay with no target molecule in the sample and (C) result of competitive immunoassay with ng amounts of target molecule in the sample; in both cases colour development at the control line (CL) confirms correct operation of the device.

detecting low molecular weight (MW) target molecules that can only accommodate one antibody binding site. Examples of low MW target molecules that have been detected in competitive lateral flow immunoassays are pesticides, hormones and drugs.[98–101] These immunoassays were carried out on nitrocellulose membranes striped with a test line of haptens (low MW antigens attached to a carrier molecule) and GNPs conjugated to reporter antibodies. When a device is inserted into the sample, liquid migrates along the strip releasing the GNPs from the conjugate pad. As they migrate towards the test line antibodies conjugated to the GNPs bind to target molecules. In the absence of any target molecules none of the antibody binding sites are occupied and GNPs bind to the test line as shown in Fig. 13B, but as the number of target molecules increases antibody binding sites are occupied and colour development decreases, until eventually the test line became colourless as shown in Fig. 13C. Recently, Wilson and colleagues have reported a new form of lateral flow device based on GNPs conjugated to antigens instead of antibodies, and showed how sensitivity can be increased beyond what is possible with traditional devices by tuning the number of recognition molecules per particle to the tipping point.[102] Non-competitive immunoassays are used to detect high MW target molecules that can accommodate at least two antibody binding sites. Examples of high MW target molecules that have been detected with lateral flow devices are prostate specific antigen,[103] ricin,[104] and *Staphylococcus aureus*.[105] These immunoassays were carried out on membranes striped with a test line of detector antibodies and GNPs conjugated to reporter antibodies. When a device is inserted into the sample GNPs are released into suspension. As the particles migrate towards the test line antibodies conjugated to them bind to target molecules. On reaching the test line target molecules bound to the particles are sandwiched between them and the detector antibodies leading to a visible increase in colour. Typical times from start to finish in both types of lateral flow assay are less than 10 min, and typical sensitivities are nanomolar for competitive immunoassays and picomolar for non-competitive.

Nucleic acid lateral flow devices

Most lateral flow devices are designed to detect antigens, but new knowledge emerging from the Human Genome Project and related programmes has emphasized the potential advantages of detecting nucleic acids. This has prompted a growing number of research groups and companies to embark on the development of nucleic acid lateral flow (NALF) devices. Most of these devices are based on a combination of PCR and the existing antibody–hapten technology that is used in lateral flow immunoassays. Hasegawa and co-workers amplified 83 base sequence from *Mycobacterium tuberculosis* with primers terminating in fluorescein and biotin, and applied the products to lateral flow devices striped with anti-fluorescein antibodies.[106] Double stranded products were sandwiched between GNPs conjugated to streptavidin and the antibodies as shown in Fig. 14A. There are many minor variations on this approach, but all of them are limited by the number of antibody–hapten combinations that are available for use with PCR. In practice this limits the number

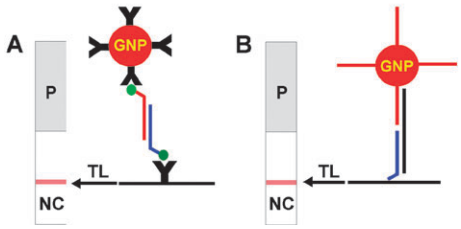

Fig. 14 (A) Section through test line (TL) of a nucleic acid lateral flow device based on antibodies and haptens (green circles). (B) Section through test line of antibody-free lateral flow device. Figure reprinted from ref. 95 by permission of The Royal Society of Chemistry (http://dx.doi.org/10.1039/b708859k).

of target molecules that can be detected with the same device to only one, at a time when there is increasing demand for devices that can detect multiple targets in the same sample.[107,108] Various strategies have been adopted in accommodating this limitation such as the interrogation of each sample with multiple single analyte devices,[109,110] but the only approach that does not lead to an increase in complexity is the elimination of antibodies and haptens from these devices altogether. Wilson and co-workers demonstrated how this can be done and detected unlabeled PCR products with an antibody-free lateral flow device that was inserted directly into these products at room temperature.[95] Target sequences were sandwiched between GNPs conjugated directly to reporter oligonucleotides and capture oligonucleotides anchored to the test line without an intervening protein anchor as shown in Fig. 14B. This approach has the potential to detect multiple target sequences on the same device, but because double stranded PCR products do not hybridise in the rapid flow environment of lateral flow devices it was necessary to interface the devices with an asymmetric PCR protocol that generated an excess of single stranded products. Unfortunately asymmetric PCR is difficult to optimise for multiple target sequences in the same sample, so the problem of how to detect multiple targets on the same lateral flow device has not been solved.

Flow through devices

In their most simple embodiment flow-through devices consist of a white porous membrane spotted with capture reagents overlying an absorbent pad as shown in Fig. 15. When a sample is applied to the device it migrates through the membrane where target molecules bind to the capture reagents and into an underlying absorbent pad. This is usually followed by a wash step and the application of labeled reporter molecules that bind to captured target molecules. In early versions the label was often an enzyme, but nowadays the most common label is GNPs.[111,112] Flow-through devices based on GNPs have been used to detect antibodies. They are often more sensitive than lateral flow devices and they are more easily adapted for the detection of multiple targets organized into two-dimensional arrays, but they are less popular than lateral flow devices because they place a greater skill-burden on the user.

Blots and arrays

Blots can be divided into those in which the sample is first resolved into its components by electrophoresis before being

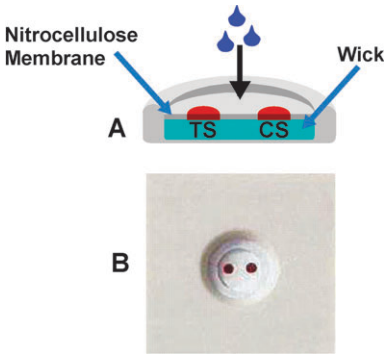

Fig. 15 (A) Schematic section through a flow through device showing locations of the test spot (TS) and control spot (CS) relative to the absorbent wick. (B) Plan view of actual device showing positive result in a non-competitive immunoassay.

blotted onto a membrane (Southern, Northern and Western blotting) and dot-blots in which the sample is spotted onto the membrane without prior separation by electrophoresis. In both types of assay the membrane is then interrogated with labeled reporter molecules, which in many cases have been GNPs conjugated to antibodies.[92,113,114] Blots are one of the precursor technologies of modern arrays. The difference is that for arrays the sample is applied to a two-dimensional grid of probe molecules instead of the other way round. For results to be easily identifiable by the unaided human eye each spot must have at least millimetre dimensions. This creates problems because the volume of sample required to irrigate an array increases in proportion to its size, whereas PCR products have volumes of around 25 microlitres and the trend here and in other techniques is to decrease this. The most common solution to this problem has been to decrease the size of the array and detect the results with some form of imaging equipment. Fritzsche and co-workers showed that arrays of 30 nm GNPs conjugated to thiolated oligonucleotides hybridised to capture probes (spot size 50 μm) on a glass substrate could be imaged with an ordinary light-microscope interfaced with a CCD camera.[115] The imaging method is relatively simple, but the sensitivity is less than obtained with fluorescence dyes. Christensen and co-workers also found lower sensitivity than fluorescence when they used arrays of haptens and GNPs conjugated to antibodies to perform competitive immunoassays for pesticides, and imaged the results with a document scanner.[116] Lahiri and co-workers used a white light CCD imaging system to detect size dependent scattering (resonance light scattering; RLS) from 80 nm GNPs.[117] Biotinylated cDNA sequences derived from human lung mRNA were sandwiched between high density arrays of capture oligonucleotides and GNPs conjugated to anti-biotin. Because the target sequences were also labeled with Cy3 it was possible to demonstrate the superiority of scattering from GNPs by direct comparison with fluorescence on the same array. The same system was also used to interrogate total (unamplified) RNA for microbial pathogens where once again its superior sensitivity ($>$50-fold) to fluorescence was demonstrated.[118]

Silver enhanced arrays

Mirkin and co-workers improved the sensitivity of arrayed detection of nucleic acids by silver enhancement.[83] Nucleic acid target sequence (corresponding to anthrax lethal factor) were sandwiched between GNPs conjugated to thiolated oligonucleotides and an array of capture probes covalently anchored to a glass substrate. After silver enhancement the arrays (spot size after enhancement 200 micrometres) were imaged with an ordinary document scanner (600 dots per inch) and analyzed with standard imaging software (Adobe Photoshop). Sensitivity was greater than when a fluorescent dye (Cy3) was used as the label, and when hybridisation was carried out at the highest stringency temperature of 50 °C selectivity for perfectly matched sequences over single base mismatches was also better. More recently the sensitivity of this approach has been improved even further by workers at Nanosphere Inc (Northbrook, IL) by automating the silver enhancement, and replacing the document scanner with an imaging system in which evanescent light from the array substrate is scattered by the silver enhanced GNPs and captured with a CCD camera.[91,119,120] This allows unamplified DNA and RNA target sequences to be detected in the presence of genomic DNA. In a typical genotyping assay genomic DNA is sheared into 300–500 base fragments and hybridised to an array of allele specific capture oligonucleotides before being labeled with GNPs conjugated to thiolated oligonucleotides as shown in Fig. 16. After washing away unbound GNPs the signal is enhanced by silver staining and then light scattering excited by evanescent coupling from the substrate interfaced with red light-emitting diodes (λ_{max} 630 nm) is quantified with a proprietary reader (Verigene ID™). Each array is scanned multiple times at various exposure times. This system can genotype multiple genes in the same sample in approximately 1 h with as little as 500 ng of input genomic DNA (the amount present in a single drop of blood). The combination of GNPs, arrays and silver staining has also been used with the ArrayTube technology developed by Clondiag Chip Technologies GmbH (Jena, Germany). Monecke and co-workers used their array-in-a-tube system to screen for antibiotic resistance in *Staphylococcus aureus*.[121] Microbial DNA was enzymatically amplified and labeled with biotin, and then hybridised to an array of specific capture oligonucleotides. Hybridisation products were labeled *in situ* with GNPs conjugated to streptavidin and then the signal was enhanced by silver staining and imaged with a proprietary CCD reader. Silver stained GNPs and arrays have also been used to detect microbial pathogens,[122] proteins (hepatitis B antibodies),[123] and to investigate the substrate specificity of kinase enzymes.[124] In the latter report arrays of peptides were contacted with a solution of the kinase and a biotinylated derivative of ATP. Biotin was transferred to peptides when they were phosphorylated and subsequently labeled with GNPs conjugated to streptavidin and silver enhanced. The silver stained arrays described above were imaged with a relatively inexpensive CCD, but this limits the size of the array spots that can be resolved and hence the number of tests that can be performed on the same chip. Much higher resolutions are possible with a confocal microarray scanner, but the cost is much higher. Bernard and colleagues got round this problem by spotting arrays of antibodies onto a disc and reading the results with a modified CD player (Fig. 17).[125] In a conventional CD player information is extracted by focussing laser light onto a disc and measuring the intensity of light reflected from a series of pits encoded into a spiral metal track as it rotates. In the modified version a similar set up was used to read information

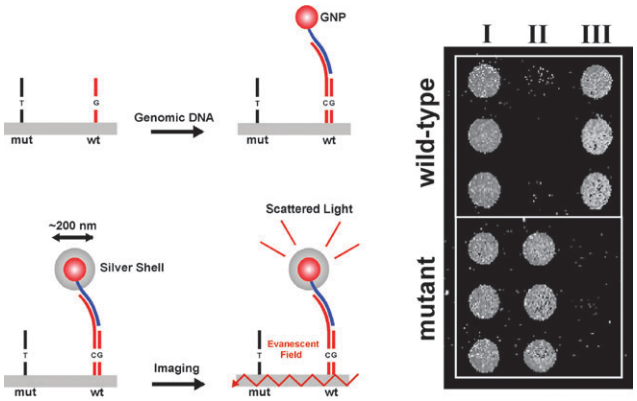

Fig. 16 (A) Schematic protocol for SNP identification in Nanosphere's Verigene system. Genomic DNA is contacted with an array of allele-specific capture probes. After removing unbound DNA, hybridization products are labelled with GNPs, and after removing unbound GNPs the array is silver enhanced and imaged in the Verigene ID imaging system. (B) 16-bit greyscale image created by the Verigene ID imaging system after genomic DNA samples of known genotype ((I) heterozygous, (II) homozygous wild-type, (III) homozygous mutant) were subjected to a 1 h assay. Array image reprinted from ref. 119 by permission of Oxford University Press.

from a series of metal spots formed by silver enhancement of antigens sandwiched between capture antibodies and reporter antibodies conjugated to GNPs. This approach combines low cost with high resolution and could be used with lab-on-a disc technology.[126]

Universal labelling systems for blots and arrays

Universal labelling systems allow arrays to be labeled without preparing a different label for each target sequence. Because the label is added after binding of the reporter molecule to the target it does not interfere with the molecular recognition events that confer specificity. Universal labels based on GNPs conjugated to recognition molecules such as streptavidin are widely used but expensive. Several companies supply universal labelling systems that stain all proteins on an array or blot. Examples are Protogold (BBInternational, Cardiff, UK) and

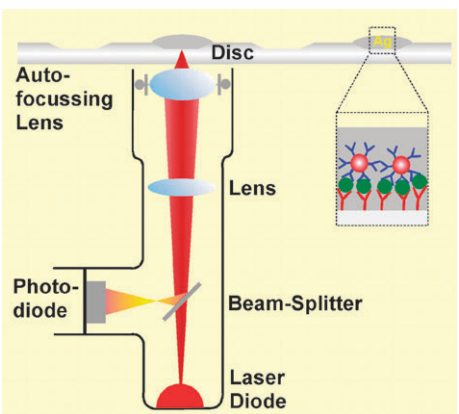

Fig. 17 Section through pick-up head and part of the disc of a CD player modified for biological detection. Light from a laser diode is directed onto the disc as it rotates and light scattered back from silver enhanced array spots is detected with a photodiode.

Colloidal Gold Total Protein Stain (BioRad, Hercules, CA) both of which bind to proteins by a combination of electrostatic and hydrophobic interactions.[127] Golovlev and co-workers have reported a universal labelling system based on electrostatic attraction between positively charged GNPs and the negatively charged backbone of double stranded DNA.[128,129] The formation of double stranded products promotes strong interactions between the phosphate backbone and 250 nm GNPs coated with a positively charged polymer. This labelling system is currently being developed by Sci-Tec (Knoxville, TN) as part of the Aurogen personalized microarray system that also includes a high performance flatbed scanner for array imaging. Mehrabi and Wilson have reported a universal labelling system for double stranded hybridisation products based on GNPs conjugated to intercalating molecules that insert specifically between the bases of double stranded nucleic acids.[88] This is less prone to interference than methods based on non-specific interactions, but low cost is retained.

Bio-barcode assays

The bio-barcode approach as first reported by Mirkin and co-workers[130,131] has subsequently been presented in several different formats. In one of its most recent versions the protocol is carried out in a disposable chip as shown in Fig. 18A.[132] Magnetic microspheres conjugated to capture antibodies are mixed with the sample and loaded onto the chip. Following an incubation period for capture of target molecules a magnet is applied under the chip to retain the microspheres while the remainder of the sample is washed away. Next GNPs conjugated to detector antibodies and double stranded oligonucleotide barcodes are flowed through the chip such that target molecules are sandwiched between the microspheres and the GNPs. After washing away unbound GNPs, DNA barcodes are released (dehybridized) by running deionised water through the chip, and then the released barcodes are sandwiched between immobilized capture oligonucleotides and reporter oligonucleotides conjugated to GNPs; note that these are not the same GNPs that were bound to the magnetic microspheres in the earlier part of the protocol. After washing away unbound GNPs the signal is enhanced by silver staining and imaged with the Verigene ID scanning system developed by Nanosphere. Attomolar concentrations of antigens can be detected, which compares favourably with fluorescence and enzyme-based detection, and approaches the sensitivity of immuno-PCR.[133] The main source of signal amplification is silver enhancement rather than the small ($\sim$2 orders of magnitude) increase that occurs when target molecules are reformatted onto DNA barcodes. Groves and co-workers increased the amount of amplification without silver enhancement by using the volume of porous silica microspheres rather than surface of GNPs as a repository for the barcodes. This allows distance dependent detection of attomolar concentrations of target molecule by the unaided eye.[134] Bio-barcode assays have also been used to detect multiple target molecules in the same sample. The way in which this is achieved is shown schematically in Fig. 18B. Target molecules are sandwiched between sets of magnetic

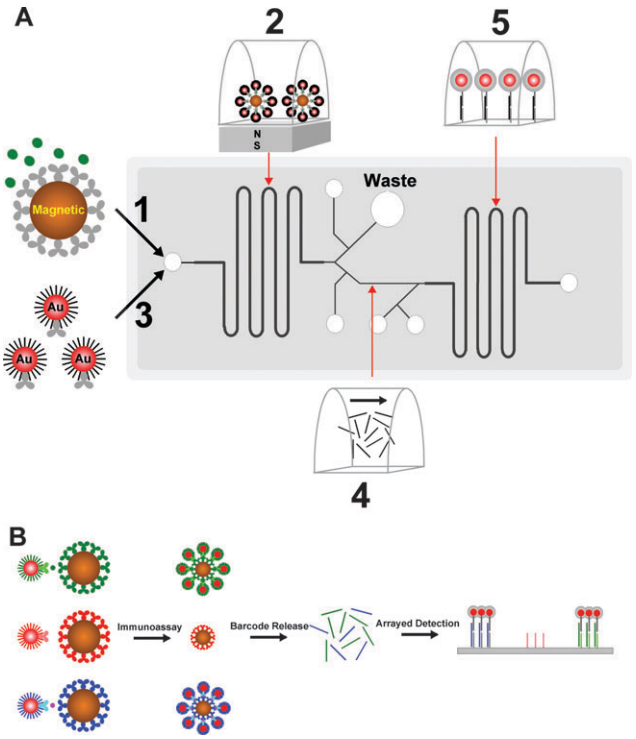

Fig. 18 (A) Biobarcode assay on a microfluidic chip. In step 1 the sample (green circles) is mixed with magnetic beads conjugated to antibodies and introduced into the separation area of the chip. In step 2 the magnetic beads are retained in the separation area by applying a magnet under the chip and unreacted sample is flowed to waste. In step 3 GNPs conjugated to antibodies and double stranded DNA barcodes are introduced into the chip and mixed with the magnetic beads. Bound target molecules are sandwiched between the magnetic beads and GNPs, and unbound GNPs are flowed to waste. In step 4 the magnetic beads are retained in the separation area and DNA barcodes are dehybridised from them by running water through the chip. In step 5 released barcodes are sandwiched between GNPs and immobilized capture probes and silver enhanced. The base of the chip is then physically separated from the fluidics and imaged. (B) Multiplexed biobarcode assays are similar to single analyte assays except that the DNA barcodes are resolved with a two-dimensional array of capture probes before silver enhancement and detection.

microspheres and GNPs encoded with barcodes, and released barcodes are resolved by hybridisation to an array of capture probes and detected after silver enhancement. For this approach to be sensitive there must be no exchange of DNA barcodes between different sets of GNPs, because this would lead to high background signals such as have in fact been detected in assays for oligonucleotides[135] and protein cancer markers.[136] The origin of these non-specific signals has not been identified, but they must be eliminated if the multiplexed biobarcode assays are to achieve the same sensitivity as the single analyte assays.

Electrical detection

The success of amperometric biosensors has demonstrated that methods based on the detection of an electric current are more suitable than any other for the acquisition of quantitative information in point-of-need applications. If molecules in a narrow gap between two electrodes are labeled with GNPs and then interconnected by deposition of metallic silver, there is a decrease in resistance that can be measured with simple and inexpensive equipment. The use of this approach for biological detection was first described in patents assigned to Mroczkowski and colleagues,[137] and later in a publication by Velev and Kaler who carried out non-competitive immunoassays for antibodies in a flow-cell overlying electrodes separated by micrometre-sized gaps.[138] A dense layer of latex microspheres coated with protein A was deposited in the gap by application of an alternating electric field and then target molecules were sandwiched between it and reporter antibodies conjugated to 5 nm GNPs. Bound particles were then enlarged and fused by catalytic deposition of silver leading to a time-dependent drop in electrical resistance in proportion to the amount of target molecule in the sample. This method of detection was later used in a fully automated platform for food-borne pathogens (Fig. 19) developed by Molecular Circuitry (King of Prussia, PA)[139] and for the arrayed detection of nucleic acids.[140–142] In one of these later reports Mirkin and colleagues demonstrated high discrimination for (10^5 : 1) SNPs,[140] and in another Fritzsche and colleagues showed how multiple nuclei acid sequences could be detected in parallel in a way that was potentially suitable for point-of-need applications.[142] The main problem with these nucleic acid sensors was that high sensitivity and broad dynamic range was only achieved by multiple cycles of silver deposition, washing, drying and measurement (10–15 cycles in the method reported by Mirkin[140]), but more recently Diessel and colleagues have shown how this can be avoided by monitoring the resistance drop in real-time.[143] Ideally the requirement for metal deposition would be eliminated altogether, but GNPs that have not been interconnected do not permit the passage of an electric current because they are not close enough together, and because they are surrounded by an insulating shell of biological molecules. Paek and colleagues attempted to overcome this by coating GNPs conjugated to antibodies with a conducting polymer that extended into the surrounding solution.[144] Particles prepared in this way were used in lateral flow devices that incorporated two interdigitated electrodes printed directly onto the chromatographic strip. Diagrams published in their report show the conducting polymer in electrical contact with the metallic gold of neighbouring particles, but antibodies conjugated to GNPs by non-specific adsorption are believed to occupy a closely packed shell surrounding the gold core that would not normally be

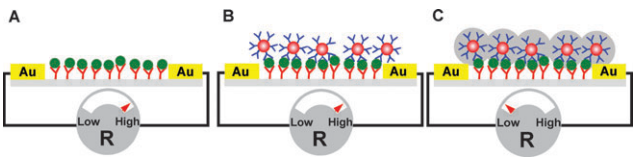

Fig. 19 (A) Antibodies immobilized in the gap between two gold electrodes capture target molecules (green circles)—electrical resistance between the electrodes is high. (B) Target molecules are sandwiched between the capture surface and reporter antibodies conjugated to GNPs—resistance is still high. (C) Catalytic deposition of metallic silver around the GNPs bridges the gap between the gold electrodes—resistance is low.

breached in this way. In addition, the polymer that was used (polyaniline) is not normally conducting at the pH that obtains in lateral flow immunoassays.

Surface-enhanced Raman scattering

Raman scattering occurs when an incoming photon enters into a virtual state with an absorbing molecule. The wavelength of the incoming photon need not correspond to an energy transition in the molecule, but when the virtual state collapses a new photon is emitted (inelastically scattered) that has a different wavelength to the original; this difference is due to an exchange of energy with a vibrational transition in the molecule. For incoming photons of a given wavelength the emission spectrum of scattered photons is highly characteristic of the absorbing molecule. Raman scattering on its own is too weak to be useful in detection, but in 1974 Fleischmann and colleagues observed enormous enhancements (10^5–10^6) from pyridine molecules adsorbed on a silver electrode that had previously been roughened by successive cycles of oxidation and reduction.[145] This surface-enhanced Raman scattering (SERS) is now known to occur when Raman active molecules are located in very close proximity to certain metal surfaces (gold and silver are the most often used) with roughness on a scale of 10–100 nm.[146] Enhancements of up to 10^{14} over unenhanced molecules have been reported, but these depend strongly on the local geometry and decrease rapidly as the distance from the metal increases; signal reductions of 90% for distance increases of only a few nanometres have been reported. Under optimum conditions sensitivity is reported to be two to three orders of magnitude better than fluorescence, but in order to achieve this interference from other molecules and ambient conditions must be eliminated. Background signals from water are very low and photobleaching is not a problem.

The two main strategies for using SERS in detection are direct identification of Raman active molecules located in close proximity to a nanostructured metal surface, and indirect detection of Raman reporter molecules that have been incorporated into a biospecific label. Often the easiest way to obtain a Raman spectrum is to adsorb the molecular species of interest onto GNPs, but although spectra produced in this way can provide useful information about molecular structure they are not particularly useful for detecting specific molecules in complex solutions, due to interference from competing adsorbates and hypersensitivity to ambient conditions. If interference from other adsorbates can be eliminated, sensitivity to ambient conditions can sometimes be exploited to monitor localized changes in the surrounding medium. Halas and colleagues assembled a monolayer of mercaptobenzoic acid on gold nanoshells and monitored changes in the Raman spectrum induced by protonation and deprotonation of the exposed carboxylic groups (Fig. 20Ai).[147] Excitation and emission were in the near infrared region where blood and tissue are least absorbing, and pH was measurable over a range that would allow discrimination between acidic cancer and healthy untransformed cells. It was suggested that nanosensors with this design could be embedded in plant and animal tissues to monitor changes in cellular or sub-cellular conditions, but improvements in design would be required to

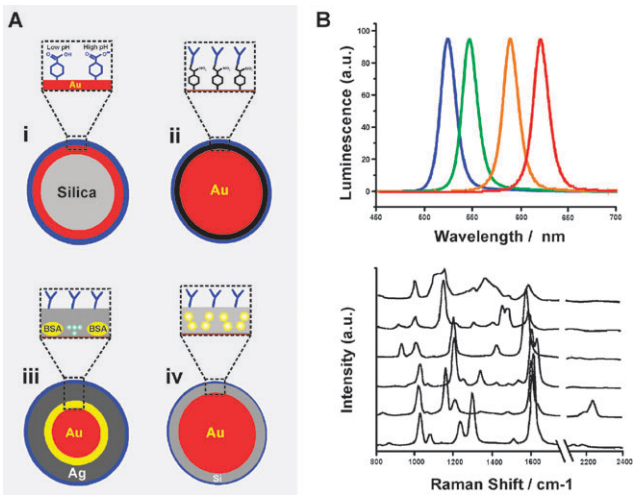

Fig. 20 (A) The evolving use of GNPs and SERS in detection: (i) Gold nanoshell functionalized with mercaptobenzoic acid for direct monitoring of pH; (ii) biospecific label with inner shell of Raman reporter molecules and outer shell of antibodies; (iii) label with GNP core, inner shell of Raman reporter molecules embedded in metallic silver and outer shell of antibodies; (iv) label with GNP core, inner shell of Raman reporter molecules encapsulated in silica and outer shell of antibodies. (B) Emission spectra of (top) CdSe/ZnS QDs and (bottom) six Raman reporter molecules used in Nanoplex biotags. QDs have been used to create up to 100 resolvable signatures, but an upper limit of only 20 has been predicted for signatures based on SERS.[157]

prevent displacement of mercaptobenzoic acid by high intracellular (millimolar) concentrations of glutathione, and interference from the electrostatic binding of proteins and other molecules to the exposed carboxylic acids.

Problems with interference from competing adsorbates and ambient conditions have motivated a move away from direct identification to the use of Raman active molecules as reporters in biospecific labels. Lipert and colleagues prepared labels consisting of 30 nm GNP cores surrounded by an inner shell of thiolated nitroaromatic molecules that were covalently attached to an outer shell of antibodies.[148] This design (Fig. 20Aii) locates a large number (10^3–10^4) of Raman active molecules in close proximity to each GNP and separates them from the recognition function provided by the antibodies. Labels with this design were used in immunoassays in which prostate specific antigen was sandwiched between them and a macroscopic gold sensing surface; picomolar concentrations were detected. Although the Raman reporters in these labels are separated from the surrounding solution by the outer shell of antibodies this probably does not isolate them from all variations in ambient conditions. Mirkin and colleagues located Raman reporters in close proximity to a metal surface by silver enhancement of GNPs.[149] Oligonucleotide target sequences were sandwiched between arrays of capture probes, and reporter probes labeled with GNPs and a Raman active organic dye such as Cy3. Before silver enhancement no Raman scattering could be detected, but after enhancement intense signals were detected due to deposition of silver around the dye molecules. Because the Raman spectrum derived mainly from the dye it could be used as a fingerprint to identify

different Raman reporters in the same array spot. The same group has used a similar approach to detect low molecular weight antigens,[150] and more recently two groups have developed biospecific labels that are conceptually similar except that silver is deposited around the reporter molecules before they are used for detection (Fig. 20Aiii).[151,152] Metallic silver is a good enhancer of SERS, but it does not provide a good surface for the conjugation of recognition molecules. Mulvaney and colleagues encapsulated GNPs and Raman reporter molecules in an outer shell of silica rather than silver (Fig. 20Aiv).[153] The silica shell entraps the molecules in close proximity to the gold and provides a versatile surface for the conjugation of recognition molecules. A similar approach was reported by Doering and Nie,[154] and more recently labels with this design have been commercialized by Oxonica (Oxford, UK). Their Nanoplex biotags comprise a 50–90 nm GNP core surrounded by a 20–50 nm thick shell of silica with entrapped reporter molecules. They produce reproducible Raman spectra in all conditions that might be encountered in biomolecular assays.

Because the Raman spectra of many different molecules can be excited at the same wavelength, and because each spectrum is unique, they can be used as signatures in multiplexed detection.[155] Each spectrum is composed of multiple bands that are individually much narrower than those of fluorescent dyes or quantum dots (QDs), but the latter usually have a single distinct emission peak. This difference (Fig. 20B) determines how they are used as signatures in multiplexed detection. Fluorescent dyes or QD signatures are prepared by encoding with different colours at different intensities. The total number of signatures that can be created is given by the formula $C = N^m - 1$ where C = the number of codes, N = the number of resolvable intensity levels and m = the number of resolvable colours). It is very difficult to prepare Raman signatures in this way because the emission peak of one molecular species almost always overlaps with the peaks of other species excited at the same wavelength. As a result Raman signatures are normally prepared by encoding each label with only one reporter molecule per signature. This limits the number of signatures that can be resolved in multiplexed detection to no more than a few dozen compared with at least 100 when QDs are used.[156] This may not be a major limitation because in many cases multiplexed detection involves the interrogation of medium sized panels of target molecules rather than large numbers. A number of companies now market portable (and in some cases handheld) Raman detectors, and these are predicted to shrink to credit card-sized in the near future. Oxonica is developing such instrumentation for use with its Nanoplex biotags and a lateral flow device that detects up to three respiratory viruses in the same sample.[157] This device is different to existing multiplexed devices that have one test line for each target molecule because it has a single line striped with three different antibodies. The sample pad contains three different biotags each conjugated to a different anti-viral antibody. If one or more of the target viruses is present in the sample colour is seen to be developed at the test line in the normal way because biotags have a GNP core, but if the test line is then interrogated with a SERS reader the viruses can also be identified and quantified.

Fig. 21 Fingerprint on polypropylene stained with gold enhanced GNPs, and imaged with an office document scanner. Image courtesy of The School of Criminal Sciences, University of Lausanne, Switzerland.

Fingerprint detection

Forensic researchers are continually trying to develop new and improved methods for detecting fingerprints on a variety of substrates. Staining with GNPs followed by catalytic enhancement with a metal offers a number of advantages in that it is very sensitive and efficient on a large number of substrates, including some that may present difficulties for other techniques such as polystrene packaging, thermal paper and wetted surfaces. The use of GNPs for fingerprint detection was introduced by Saunders,[158] and later improved by Schnetz and Margot.[159] When a substrate bearing a latent fingerprint is immersed in colloidal gold at low pH the particles become bound to the print by a mechanism that is believed to involve electrostatic attraction. Bound particles are then enhanced by catalytic deposition of metallic silver. Recently Stauffer and co-workers have further simplified the method and reduced the cost by enhancing the bound particles with gold instead of silver (Fig. 21),[160] and Becue and co-workers have shown how prints can be stained with coloured dyes hosted by GNPs conjugated to cyclodextrins.[161]

Golden future

Although GNPs continue to be one of the most widely used labels in diagnostics, the level of sensitivity that is desirable in many diagnostic tests is greater than the sensitivity with which GNPs can be detected by the unaided eye. This has prompted the introduction of alternative labels,[162,163] but because these require expensive detection equipment they relinquish one of the key advantages that have made GNPs so successful. The minimum number of GNPs that can be detected with the unaided eye on a white background is around 1×10^{10}. If each particle in this amount corresponds to one molecule the amount of target molecule that can be detected is 10 femtomoles, but the amount likely to be present in a typical biopsy sample is one million times less than this. There is therefore, a

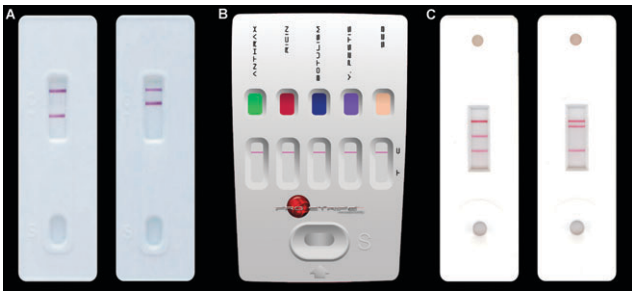

Fig. 22 Multiplexed lateral flow devices based on GNPs. (A) Serial detection of up to four cardiac markers; courtesy of BioAssay Works, Ijamsville, MD. (B) Parallel detection of up to five threat agents; courtesy of Advnt Biotechnologies, Phoenix, AZ. (C) Serial detection of up to six amplified nucleic acid targets; courtesy of BBInternational, Cardiff, UK.

significant gap between what can be detected and what actually needs to be detected in real samples. This gap can be bridged by combining GNPs with some form of amplification technique such as PCR or metal enhancement. PCR can amplify the amount of nucleic acid target molecules in a biopsy sample to nanomolar concentrations, which is well within the detection range of GNPs, but not of most other labels that can be seen with the unaided eye. This property of being able to reach down and render visible the products of amplification techniques such as PCR is why GNPs are likely to remain important in diagnostics and detection for the foreseeable future. The amplification method need not be PCR: several research group have reported alternative techniques, including Groves and co-workers who have shown how a combination of barcoded amplification and distance dependent detection permits attomole amounts of cytokines to be detected with the unaided eye.[134] The main disadvantage of these alternatives in their current embodiments is their inability to detect more than one target molecule at a time when information emerging from the Human Genome Project and related programmes is emphasizing the advantages of being able to detect multiple targets in the same sample. In response to this trend a number of research groups have investigated the combination of silver enhancement and arrayed detection, most notably workers at Northwestern University, and their spin-off company Nanosphere, which has combined it with a relatively inexpensive imaging platform. The genetic tests sold by this company are the first major diagnostic products to emerge from the heightened interest in GNPs that began in the middle of the last decade. Lateral flow detection has responded to demands for higher levels of multiplexing by introducing devices that can detect multiple targets in the same sample as shown in Fig. 22. This trend is likely to continue with devices that combine the serial and parallel formats shown in this figure being used to interrogate medium sized panels of several dozen targets molecules such as are important in the diagnosis and prognosis of disease, and in the administration of targeted therapies. Multiple nucleic acid targets can be detected by interfacing lateral flow devices with nucleic acid amplification techniques as shown in Fig. 22C, but protein targets are more difficult because they are less amenable to amplification. Sensitivity can be increased by post-lateral flow silver-enhancement[164] and other strategies,[165] but because these involve additional steps that must be performed by the user they depart form the model that has made lateral flow devices so successful. Mirkin and co-workers have shown how attomole amounts of non-nucleic acid targets can be detected in a microfluidic device by barcoded detection and silver enhancement,[132] and potentially this approach could be extended to multiple protein and nucleic acid targets, but there are continuing doubts about the affordability of microfluidic devices, especially in settings such as developing countries where they are most needed.[166] During the last decade researchers have harnessed the unique properties of GNPs for an ever increasing diversity of detection methods. The challenge now is to transform these methods into inexpensive tests that allow untrained users to detect low concentrations of multiple targets in real samples.

References

1 C. F. A. Lange, *Berl. Klin. Wochenschr.*, 1912, **49**, 897.
2 F. Green, *Can. Med. Assoc. J.*, 1925, **15**, 1139.
3 W. P. Faulk and G. M. Taylor, *Immunochemistry*, 1971, **8**, 1081.
4 J. W. Slot and H. J. Geuze, *Eur. J. Cell Biol.*, 1985, **38**, 87.
5 G. W. Hacker, L. Grimelius, G. Danscher, G. Bernatzky, W. Muss, H. Adam and J. Thurner, *J. Histotechnol.*, 1988, **11**, 213.
6 P. M. Lackie, *Histochem. Cell Biol.*, 1996, **106**, 9.
7 T. Ung, L. M. Liz-Marzan and P. Mulvaney, *J. Phys. Chem. B*, 2001, **105**, 3441.
8 J. H. W. Leuvering, P. J. H. M. Thal, M. V. D. van der Waart and A. H. W. M. Schuurs, *Fresenius' J. Anal. Chem.*, 1980, **301**, 132.
9 J. H. W. Leuvering, P. J. H. M. Thal, M. van der Waart and A. H. W. M. Schuurs, *J. Immunol. Methods*, 1981, **45**, 183.
10 J. H. W. Leuvering, B. C. Goverde, P. J. H. M. Thal and A. H. W. M. Schuurs, *J. Immunol. Methods*, 1983, **60**, 9.
11 C. X. Zhang, Y. Zhang, X. Wang, Z. M. Tang and Z. H. Lu, *Anal. Biochem.*, 2003, **320**, 136.
12 N. G. Khlebtsov, V. A. Bogatyrev, A. G. Melnikov, L. A. Dykman, B. N. Khlebtsov and Y. M. Krasnov, *J. Quant. Spectrosc. Radiat. Transfer*, 2004, **89**, 133.
13 J. H. W. Leuvering, P. J. H. M. Thal, D. D. White and A. H. W. M. Schuurs, *J. Immunol. Methods*, 1983, **62**, 163.
14 K. Aslan, J. R. Lakowicz and C. D. Geddes, *Anal. Biochem.*, 2004, **330**, 145.
15 H. Otsuka, Y. Akiyama, Y. Nagasaki and K. Kataoka, *J. Am. Chem. Soc.*, 2001, **123**, 8226.
16 M. Holtzhauer and M. Rudolph, *J. Chromatogr.*, 1992, **605**, 193.
17 T. C. J. Gribnau, J. H. W. Leuvering and H. van Hell, *J. Chromatogr., Biomed. Appl.*, 1986, **376**, 175.
18 P. Englebienne, A. Van Hoonacker and J. Valsamis, *Clin. Chem. (Washington, D. C.)*, 2000, **46**, 2000.
19 P. Englebienne, A. Van Hoonacker and M. Verhas, *Spectroscopy (Amsterdam)*, 2003, **17**, 255.
20 L. R. Hirsch, J. B. Jackson, A. Lee, N. J. Halas and J. West, *Anal. Chem.*, 2003, **75**, 2377.
21 R. Elghanian, J. J. Storhoff, R. C. Mucic, R. L. Letsinger and C. A. Mirkin, *Science*, 1997, **277**, 1078.
22 J. J. Storhoff, R. Elghanian, R. C. Mucic, C. A. Mirkin and R. L. Letsinger, *J. Am. Chem. Soc.*, 1998, **120**, 1959.
23 J. J. Storhoff, A. A. Lazarides, R. C. Mucic, C. A. Mirkin, R. C. Letsinger and G. C. Schatz, *J. Am. Chem. Soc.*, 2000, **122**, 4640.
24 R. C. Jin, G. S. Wu, Z. Li, C. A. Mirkin and G. C. Schatz, *J. Am. Chem. Soc.*, 2003, **125**, 1643.
25 T. A. Taton, G. Lu and C. A. Mirkin, *J. Am. Chem. Soc.*, 2001, **123**, 5164.
26 D. Murphy and G. Redmond, *Anal. Bioanal. Chem.*, 2005, **381**, 1122.
27 D. Murphy, P. O'Brien and G. Redmond, *Analyst*, 2004, **129**, 970.
28 M. Liew, R. Pryor, R. Palais, C. Meadows, M. Erali, E. Lyon and C. Wittwer, *Clin. Chem. (Washington, D. C.)*, 2004, **50**, 1156.

29 G. H. Reed, J. O. Kent and C. T. Wittwer, *Pharmacogenomics*, 2007, **8**, 597.
30 J. H. Li, X. Chu, Y. L. Liu, J. H. Jiang, Z. He, Z. Zhang, G. L. Shen and R. Q. Yu, *Nucleic Acids Res*., 2005, **33**, e168.
31 W. J. Qin and L. Y. L. Yung, *Nucleic Acids Res*., 2007, **35**, e111.
32 S. R. Nicewarner-Pena, S. Raina, G. P. Goodrich, N. V. Fedoroff and C. D. Keating, *J. Am. Chem. Soc*., 2002, **124**, 7314.
33 A. R. Herdt, S. M. Drawz, Y. J. Kang and T. A. Taton, *Colloids Surf., B*, 2006, **51**, 130.
34 R. L. Letsinger, R. Elghanian, G. Viswanadham and C. A. Mirkin, *Bioconjugate Chem*., 2000, **11**, 289.
35 Z. Li, R. C. Jin, C. A. Mirkin and R. L. Letsinger, *Nucleic Acids Res*., 2002, **30**, 1558.
36 J. A. Dougan, C. Karlsson, W. E. Smith and D. Graham, *Nucleic Acids Res*., 2007, **35**, 3668.
37 A. B. Chan and J. D. Fox, *Rev. Med. Microbiol*., 1999, **10**, 185.
38 E. Tan, J. Wong, D. Nguyen, Y. Zhang, B. Erwin, L. K. Van Ness, S. M. Baker, D. J. Galas and A. Niemz, *Anal. Chem*., 2005, **77**, 7984.
39 E. Tan, B. Erwin, S. Dames, K. Voelkerding and A. Niemz, *Clin. Chem. (Washington, D. C.)*, 2007, **53**, 2017.
40 R. Stoltenburg, C. Reinemann and B. Strehlitz, *Biomol. Eng*., 2007, **24**, 381.
41 V. Pavlov, Y. Xiao, B. Shlyahovsky and I. Willner, *J. Am. Chem. Soc*., 2004, **126**, 11768.
42 C. C. Huang, Y. F. Huang, Z. H. Cao, W. H. Tan and H. T. Chang, *Anal. Chem*., 2005, **77**, 5735.
43 J. Liu and Y. Lu, *Angew. Chem., Int. Ed*., 2006, **45**, 90.
44 C. Guarise, L. Pasquato, V. De Filippis and P. Scrimin, *Proc. Natl. Acad. Sci. U. S. A*., 2006, **103**, 3978.
45 Z. X. Wang, R. Lévy, D. G. Fernig and M. Brust, *J. Am. Chem. Soc*., 2006, **128**, 2214.
46 J. C. Achenbach, W. Chiuman, R. P. G. Cruz and Y. Li, *Curr. Pharm. Biotechnol*., 2004, **5**, 321.
47 J. Liu and Y. Lu, *J. Am. Chem. Soc*., 2004, **126**, 12298.
48 W. A. Zhao, W. Chiuman, J. C. F. Lam, M. A. Brook and Y. F. Li, *Chem. Commun*., 2007, 3729.
49 K. Sato, K. Hosokawa and M. Maeda, *J. Am. Chem. Soc*., 2003, **125**, 8102.
50 K. Sato, M. Onoguchi, Y. Sato, K. Hosokawa and M. Maeda, *Anal. Biochem*., 2006, **350**, 162.
51 W. A. Zhao, W. Chiuman, M. A. Brook and Y. F. Li, *ChemBioChem*, 2007, **8**, 727.
52 H. Li and L. Rothberg, *Proc. Natl. Acad. Sci. U. S. A*., 2004, **101**, 14036.
53 H. Li and L. Rothberg, *J. Am. Chem. Soc*., 2004, **126**, 10958.
54 H. Li and L. Rothberg, *Anal. Chem*., 2005, **77**, 6229.
55 M. Zayats, R. Baron, I. Popov and I. Willner, *Nano Lett*., 2005, **5**, 21.
56 R. Baron, M. Zayats and I. Willner, *Anal. Chem*., 2005, **77**, 1566.
57 V. Pavlov, Y. Xiao and I. Willner, *Nano Lett*., 2005, **5**, 649.
58 M. Malmqvist, *Biochem. Soc. Trans*., 1999, **27**, 335.
59 L. A. Lyon, M. D. Musick, P. C. Smith, B. D. Reiss, D. J. Pena and M. J. Natan, *Sens. Actuators, B*, 1999, **54**, 118.
60 L. He, M. D. Musick, S. R. Nicewarner, F. G. Salinas, S. J. Benkovic, M. J. Natan and C. D. Keating, *J. Am. Chem. Soc*., 2000, **122**, 9071.
61 X. C. Zhou, S. J. O'Shea and S. F. Y. Li, *Chem. Commun*., 2000, 953.
62 M. Su, S. U. Li and V. P. Dravid, *Appl. Phys. Lett*., 2003, **82**, 3562.
63 W. P. Hu, S. J. Chen, K. T. Huang, J. H. Hsu, W. Y. Chen, G. L. Chang and K. A. Lai, *Biosens. Bioelectron*., 2004, **19**, 1465.
64 P. Englebienne, *Analyst*, 1998, **123**, 15699.
65 P. Englebienne, A. V. Van Hoonacker and M. Verhas, *Analyst*, 2001, **126**, 1645.
66 M. M. Miller and A. A. Lazarides, *J. Phys. Chem. B*, 2005, **109**, 21556.
67 G. J. Nusz, S. M. Marinakos, A. C. Curry, A. Dahlin, F. Hok, A. Wax and A. Chilkoti, *Anal. Chem*., 2008, **80**, 984.
68 N. Nath and A. Chilkoti, *Anal. Chem*., 2002, **74**, 504.
69 A. Bossi, F. Bonini, A. P. F. Turner and S. A. Piletsky, *Biosens. Bioelectron*., 2007, **22**, 1131.
70 J. Matsui, K. Akamatsu, S. Nishiguchi, D. Miyoshi, H. Nawafune, K. Tamaki and N. Sugimoto, *Anal. Chem*., 2004, **76**, 1310.
71 J. Matsui, K. Akamatsu, N. Hara, D. Miyoshi, H. Nawafune, K. Tamaki and N. Sugimoto, *Anal. Chem*., 2005, **77**, 4282.
72 R. T. Ranasinghe and T. Brown, *Chem. Commun*., 2005, 5487–5502.
73 P. C. Ray, G. K. Darbha, A. Ray, J. Walker and W. Hardy, *Plasmonics*, 2007, **2**, 173.
74 E. Dulkeith, M. Ringler, T. A. Klar, J. Feldmann, A. M. Javier and W. J. Parak, *Nano Lett*., 2005, **5**, 585.
75 T. Pons, I. L. Medintz, K. E. Sapsford, S. Higashiya, A. F. Grimes, D. S. English and H. Mattousssi, *Nano Lett*., 2007, **7**, 3157.
76 E. Dulkeith, A. C. Morteani, T. Niedereicholz, T. A. Klar, J. Feldmann, S. A. Levi, F. C. J. M. van Veggel, D. N. Reinhoudt, M. Moller and D. I. Gittins, *Phys. Rev. Lett*., 2002, **89**, 203002.
77 B. Dubertret, M. Calame and A. J. Libchaber, *Nat. Biotechnol*., 2001, **19**, 365.
78 N. C. Cady, A. D. Strickland and C. A. Batt, *Mol. Cell. Probes*, 2007, **21**, 116.
79 E. Oh, M. Y. Hong, D. Lee, S. H. Nam, H. C. Yoon and H. S. Kim, *J. Am. Chem. Soc*., 2005, **127**, 3270.
80 L. M. Ao, F. Gao and B. F. Pan, *Anal. Chem*., 2006, **78**, 1104.
81 C. C. You, O. R. Miranda, B. Gider, P. S. Ghosh, I. B. Kim, B. Erdogan, S. A. Krovi, U. H. F. Bunz and V. M. Rotello, *Nat. Nanotechnol*., 2007, **2**, 318.
82 A. Arditi and K. Knoblauch, in *Functional Assessment of Low Vision*, ed. R. Cole and B. Rosenthal, Mosby Co., St. Louis, 1996, p. 129135.
83 T. A. Taton, C. A. Mirkin and R. L. Letsinger, *Science*, 2000, **289**, 1757.
84 Z. Ma and S. F. Sui, *Angew. Chem., Int. Ed*., 2002, **41**, 2176.
85 R. A. Reynolds, C. A. Mirkin and R. L. Letsinger, *Pure Appl. Chem*., 2000, **72**, 229.
86 R. Wilson, Y. Chen and J. Aveyard, *Chem. Commun*., 2004, 1156.
87 Y. Chen, J. Aveyard and R. Wilson, *Chem. Commun*., 2004, 2804.
88 M. Mehrabi and R. Wilson, *Small*, 2007, **3**, 1491.
89 P. Upadahyay, M. Hanif and S. Bhaskar, *Clin. Microbiol. Infect*., 2006, **12**, 1118–1122.
90 R. Wilson, *Chem. Commun*., 2003, 108.
91 J. J. Storhoff, S. S. Marla, P. Bao, S. Hagenow, H. Mehta, A. Lucas, V. Garimella, T. Patno, W. Buckingham, W. Cork and U. R. Müller, *Biosens. Bioelectron*., 2004, **19**, 875.
92 M. Moeremans, G. Daneels, A. Van Dijck, G. Langanger and J. De Mey, *J. Immunol. Methods*, 1984, **74**, 353.
93 K. Glynou, P. C. Ioannou, T. K. Christopoulous and V. Syriopoulou, *Anal. Chem*., 2003, **75**, 4155.
94 S. Deborggraeve, F. Claes, T. Laurent, P. Mertens, T. Leclipteux, J. C. Dujardin, P. Herdewijn and P. Buscher, *J. Clin. Microbiol*., 2006, **44**, 2884.
95 J. Aveyard, M. Mehrabi, A. Cossins, H. Braven and R. Wilson, *Chem. Commun*., 2007, 4251.
96 A. J. Verkleij and J. L. M. Leunissen, *Immuno-gold labelling in cell biology*, CRC Press, Boca Raton, FL, 1989.
97 N. R. Kramarcy and R. Sealock, *J. Histochem. Cytochem*., 1991, **39**, 37.
98 L. Q. Liu, C. F. Peng, Z. Y. Jin and C. L. Xu, *Biomed. Chromatogr*., 2007, **21**, 861.
99 C. Zhang, Y. Zhang and S. Wang, *J. Agric. Food Chem*., 2006, **54**, 2502.
100 G. P. Zhang, X. N. Wang, J. F. Yang, Y. Y. Yang, G. X. Xing, Q. M. Li, D. Zhao, S. J. Chai and J. Q. Guo, *J. Immunol. Methods*, 2006, **312**, 27.
101 B. S. Delmulle, S. M. D. G. De Saeger, L. Sibanda, I. Barna-Vetro and C. H. Van Peteghem, *J. Agric. Food Chem*., 2005, **53**, 3364.
102 J. Aveyard, P. Nolan and R. Wilson, *Anal. Chem*., 2008, **80**, 6000.
103 C. Fernàndez-Sànchez, C. J. McNeil, K. Rawson, O. Nilsson, H. Y. Leung and V. Gnanapragasam, *J. Immunol. Methods*, 2005, **307**, 1.
104 R. H. Shyu, H. F. Shyu, H. W. Liu and S. S. Tang, *Toxicon*, 2002, **40**, 255.
105 S. H. Huang, H. C. Wei and Y. C. Lee, *Food Control*, 2007, **18**, 893.
106 T. Suzuki, M. Tanaka, S. Otani, S. Matsuura, Y. Sakaguchi, T. Nishimura, A. Ishizaka and N. Hasegawa, *Diagn. Microbiol. Infect. Dis*., 2006, **56**, 275.

107 W. K. Fong, Z. Modrusan, J. P. McNevin, J. Marostenmaki, B. Zin and F. Bekkaoui, *J. Clin. Microbiol.*, 2000, **38**, 2525.
108 Y. Matsubara and S. Kure, *Hum. Mutat.*, 2003, **22**, 166.
109 D. P. Kalogianni, V. Bravou, T. K. Christopoulos, P. C. Ioannou and N. C. Zoumbos, *Nucleic Acids Res.*, 2007, **35**, e23.
110 D. P. Kalogianni, S. Goura, A. J. Aletras, T. K. Christopoulos, M. G. Chanos, M. Chrisofidou, A. Skoutelis, P. C. Ioannou and E. Panagiotopoulos, *Anal. Biochem.*, 2007, **361**, 169.
111 L. K. V. Baskar, T. R. Srikanth, S. Suba, H. C. Mody, P. K. Desai and P. Kaliraj, *Microbiol. Immunol.*, 2004, **48**, 519.
112 S. Wang, C. Zhang, J. P. Wang and Y. Zhang, *Anal. Chim. Acta*, 2005, **546**, 161.
113 D. Brada and J. Roth, *Anal. Biochem.*, 1984, **142**, 79.
114 S. Matsuzawa, H. Kimura, Y. Itoh, H. Wang and T. Nakagawa, *J. Forensic Sci.*, 1993, **38**, 448.
115 J. Reichert, A. Csáki, J. M. Köhler and W. Fritzsche, *Anal. Chem.*, 2000, **72**, 6025.
116 A. P. Han, M. Dufva, E. Belleville and C. B. V. Christensen, *Lab Chip*, 2003, **3**, 329.
117 P. Bao, A. G. Frutos, C. Greef, J. Lahiri, U. Muller, T. C. Peterson, L. Warden and X. Y. Xie, *Anal. Chem.*, 2002, **74**, 1792.
118 P. Francois, M. Bento, P. Vaudaux and J. Schrenzel, *J. Microbiol. Methods*, 2003, **55**, 755.
119 Y. P. Bao, M. Huber, T. F. Wei, S. S. Marla, J. J. Storhoff and U. R. Müller, *Nucleic Acids Res.*, 2005, **33**, e15.
120 M. Huber, T. F. Wei, U. R. Müller, P. A. Lefebvre, S. S. Marla and Y. P. Bao, *Nucleic Acids Res.*, 2004, **32**, e137.
121 S. Monecke, I. Leube and R. Ehricht, *Genome Lett.*, 2003, **2**, 106.
122 I. Alexandre, S. Hamels, S. Dufour, J. Collet, N. Zammatteo, F. De Longueville, J. L. Gala and J. Remacle, *Anal. Biochem.*, 2001, **295**, 1.
123 L. L. Duan, Y. F. Wang, S. S. C. Li, Z. X. Wan and J. X. Zhai, *BMC Infect. Dis.*, 2005, **5**, 53.
124 Z. X. Wang, J. Lee, A. R. Cossins and M. Brust, *Anal. Chem.*, 2005, **77**, 5770.
125 S. A. Lange, G. Roth, S. Wittemann, T. Lacoste, A. Vetter, J. Grassle, S. Kopta, M. Kolleck, B. Breitinger, M. Wick, J. K. H. Horber, S. Dubel and A. Bernard, *Angew. Chem., Int. Ed.*, 2006, **45**, 270.
126 M. Madou, J. Zoval, G. Y. Jia, H. Kido, J. Kim and N. Kim, *Annu. Rev. Biomed. Eng.*, 2006, **8**, 601.
127 R. Rohringer and D. W. Holden, *Anal. Biochem.*, 1985, **144**, 118.
128 Y. Sun, W. H. Fan, M. P. McCann and V. Golovlev, *Anal. Biochem.*, 2005, **345**, 312.
129 Y. Sun, K. B. Jacobson and V. Golovlev, *Anal. Biochem.*, 2007, **361**, 244.
130 J. M. Nam, C. S. Thaxton and C. A. Mirkin, *Science*, 2003, **301**, 1884.
131 J. M. Nam, S. I. Stoeva and C. A. Mirkin, *J. Am. Chem. Soc.*, 2004, **126**, 5932.
132 E. D. Goluch, J. M. Nam, D. G. Georganopoulou, T. N. Chiesl, K. A. Shaikh, K. S. Ryu, A. E. Barron, C. A. Mirkin and C. Liu, *Lab Chip*, 2006, **6**, 1293.
133 U. R. Müller, *Mol. BioSyst.*, 2006, **2**, 470.
134 J. M. Nam, A. R. Wise and J. T. Groves, *Anal. Chem.*, 2005, **77**, 6985.
135 S. L. Stoeva, J. S. Lee, C. S. Thaxton and C. A. Mirkin, *Angew. Chem., Int. Ed.*, 2006, **45**, 3303.
136 S. L. Stoeva, J. S. Lee, J. E. Smith, S. T. Rosen and C. A. Mirkin, *J. Am. Chem. Soc.*, 2006, **128**, 8378.
137 S. J. Mroczkowski, K. A. Siegesmund and D. E. Yorde, WO 90/05300, 1990.
138 O. D. Velev and E. W. Kaler, *Langmuir*, 1999, **15**, 3693.
139 S. Brunelle, *IVD Technology*, 2001, **7**, 55–66.
140 S. Park, T. A. Taton and C. A. Mirkin, *Science*, 2002, **295**, 1503.
141 R. Moller, A. Csaki, J. M. Kohler and W. Fritzsche, *Langmuir*, 2001, **17**, 5426.
142 M. Urban, R. Moller and W. Fritzsche, *Rev. Sci. Instrum.*, 2003, **74**, 1077.
143 E. Diessel, K. Grothe, H. M. Siebert, B. D. Warner and J. Burmeister, *Biosens. Bioelectron.*, 2004, **19**, 1229.
144 J. H. Kim, J. H. Cho, G. S. Cha, C. W. Lee, H. B. Kim and S. H. Paek, *Biosens. Bioelectron.*, 2000, **14**, 907.
145 M. Fleischmann, P. J. Hendra and A. J. McQuillan, *Chem. Phys. Lett.*, 1974, **26**, 163.
146 M. D. Porter, R. J. Lipert, L. M. Siperko, G. Wang and A. Narayanan, *Chem. Soc. Rev.*, 2008, **37**, 1001.
147 S. W. Bishnoi, C. J. Rozell, C. S. Levin, M. K. Gheith, B. R. Johnson, D. H. Johnson and N. J. Halas, *Nano Lett.*, 2006, **6**, 1687.
148 D. S. Grubisha, R. J. Lipert, H. Y. Park, J. Driskell and M. D. Porter, *Anal. Chem.*, 2003, **75**, 5936.
149 Y. C. Cao, R. C. Jin and C. A. Mirkin, *Science*, 2002, **297**, 1536.
150 Y. C. W. Cao, R. C. Jin, J. M. Nam, C. S. Thaxton and C. A. Mirkin, *J. Am. Chem. Soc.*, 2003, **125**, 14676.
151 X. Su, J. Zhang, L. Sun, T. W. Koo, S. Chan, N. Sundararajan, M. Yamakawa and A. A. Berlin, *Nano Lett.*, 2005, **5**, 49.
152 S. Lee, S. Kim, J. Choo, S. Y. Shin, Y. H. Lee, H. Y. Choi, S. H. Ha, K. H. Kang and C. H. Oh, *Anal. Chem.*, 2007, **79**, 916.
153 S. P. Mulvaney, M. D. Musick, C. D. Keating and M. J. Natan, *Langmuir*, 2003, **19**, 4784.
154 W. E. Doering and S. M. Nie, *Anal. Chem.*, 2003, **75**, 6171.
155 R. Wilson, A. R. Cossins and D. G. Spiller, *Angew. Chem., Int. Ed.*, 2006, **45**, 6104.
156 P. S. Eastman, W. M. Ruan, M. Doctolero, R. Nuttall, G. De Feo, J. S. Park, J. S. F. Chu, P. Cooke, J. W. Gray, S. Li and F. Q. F. Chen, *Nano Lett.*, 2006, **6**, 1059.
157 W. E. Doering, M. E. Piotti, M. J. Natan and R. G. Freeman, *Adv. Mater.*, 2007, **19**, 3100.
158 G. Saunders, *74th Annual Educational Conference*, Pensacola, USA, June 1989.
159 B. Schnetz and P. Margot, *Forensic Sci. Int.*, 2001, **118**, 21.
160 E. Stauffer, A. Becue, K. V. Singh, K. R. Thampi, C. Champod and P. Margot, *Forensic Sci. Int.*, 2007, **168**, e5.
161 A. Becue, C. Champod and P. Margot, *Forensic Sci. Int.*, 2007, **168**, 169.
162 D. Malamud, H. Bau, S. Niedbala and P. Corstjens, *Adv. Dent. Res.*, 2005, **18**, 12.
163 J. Li, K. Zhao, X. Hong, H. Yuan, L. Ma, J. Li, Y. Bai and T. Li, *Colloids Surf., B*, 2005, **40**, 179.
164 D. J. Chiao, R. H. Shyu, C. S. Hu, H. Y. Chiang and S. S. Tang, *J. Chromatogr., B: Anal. Technol. Biomed. Life Sci.*, 2004, **809**, 37.
165 R. Tanaka, T. Yuhi, N. Nagatani, T. Endo, K. Kerman, Y. Takamura and E. Tamiya, *Anal. Bioanal. Chem.*, 2006, **385**, 1414.
166 P. Yager, T. Edwards, E. Fu, K. Helton, K. Nelson, M. R. Tam and B. H. Weigl, *Nature*, 2006, **442**, 412.